General Disclaimer

One or more of the Following Statements may affect this Document

- This document has been reproduced from the best copy furnished by the organizational source. It is being released in the interest of making available as much information as possible.

- This document may contain data, which exceeds the sheet parameters. It was furnished in this condition by the organizational source and is the best copy available.

- This document may contain tone-on-tone or color graphs, charts and/or pictures, which have been reproduced in black and white.

- This document is paginated as submitted by the original source.

- Portions of this document are not fully legible due to the historical nature of some of the material. However, it is the best reproduction available from the original submission.

The Application of the Scanning Electron Microscope to Studies of Current Multiplication, Avalanche Breakdown and Thermal Runaway

(III) Thermal Runaway in multi-emitter Power Transistors

by

D. V. Sulway and P. R. Thornton,
School of Engineering Science,
University College of North Wales,
Dean Street, Bangor,
Caerns., U.K.

Grant NGR-52-117-001

Application 3. Thermal runaway in multi-finger power transistors.

1. Introduction

In a previous report (1) we outlined the ways in which the dependence of avalanche processes upon temperature may be made to give information about thermal effects in transistors. In this report we describe the application of the SEM to the study of thermal effects under non avalanching conditions. The device studied is a developmental high frequency, silicon-planar, power transistor, which is subject to 'thermal jumps' above a certain power dissipation. To be specific the device is the developmental XK523 made by STC Footscray. If the emitter current is gradually increased with a constant collector base voltage, V_{cb}, a sudden decrease of about 50mV occurs in the emitter base voltage, V_{eb}. When the emitter current is subsequently reduced V_{eb} will suddenly increase to its previous value at an emitter current slightly below that at which it fell initially. At relatively low collector base voltages this change is reversible and no degradation of the device occurs provided the sink temperature is kept low. If the collector base voltage is increased too much or the sink temperature allowed to rise permanent damage can result. The current at which this effect occurred varies from one device to another.

A working model of this effect can be summed up by saying that the 'thermal jump' represented by the sudden decrease in V_{eb} represents an initial reversible stage in the build-up of a hot spot which leads first, to current crowding and, finally, to irreversible thermal runaway.

This affect represents a reliability problem of some generality as the physical mechanisms involved are also important in second breakdown. This problem is one in which the scanning electron microscope can, in principle, be used to complement electrical measurements. However, if this technique is to be applied to problems of this nature, it has to be extended in the sense that new temperature sensitive contrast mechanisms have to be established, pulse techniques have to be applied to problems of this nature, and the stability and safety of devices operating at high currents have to be considered. The following sections describe the experience gained in this type of work. After an initial description of the experimental method used, the report describes first the results of a search for a temperature dependent contrast which is operative under non avalanching conditions and then outlines an

attempt to observe 'hot spots' directly in the SEM using a water cooled stage. The report also describes a study of the mechanical defects built-in the device. Included in the work is a discussion of initial confirmatory measurements made on other devices to establish either the correct interpretation of the results described or to illustrate the generality of the results. As the work was incomplete at the time of writing this report, it should be regarded as a progress report rather than a completed study.

2. Experimental methods

2(a) SEM studies

The devices used had the configuration shown in figure 1(a) and were mounted in TO3 headers which were, in turn, mounted on a heavy-duty heat sink. It was found necessary to provide a water-cooled specimen stage for the SEM in order to keep the sink temperature low while the device was dissipating up to 30 watts in the SEM vacuum chamber. The circuits used to examine the device in the SEM are shown in figures 1(b) and (c). Using these circuits it was possible to examine the charge collection behaviour at the emitter-base and base-collector junctions as a function of bias and current level. To obtain some indication of the relative temperature we monitored the value of

V_{eb} required to give a certain emitter current. Most of the initial work was done using the circuit shown in figure 1(c). After an examination of the device to determine the nature and extent of any mechanical faults present the following types of studies were made:-

A. Before the occurrence of the thermal jump;

(1) A given emitter current is passed through the device until V_{eb}, which is continuously monitored, has dropped to a constant value. Then a micrograph is taken of the device with the current flowing through the device.

(2) The current is then removed and the temperature allowed to drop. V_{eb} is monitored. When V_{eb} has risen to a suitable value a micrograph is taken with the emitter-base junction shorted. Afterwards V_{eb} is measured again and a mean value of V_{eb} corresponding to the micrograph was therefore obtained.

(3) Once a general picture had been obtained by taking suitable micrographs more detailed studies were made by use of line scans, in which the electron beam is constrained to scan along a preselected line and the resultant charge collection signal fed to the axis of an xy recorder while the distance signal is fed to the x axis.

In this way plots of the charge collection current, I_{cc}, as a function of distance can be obtained and compared with infra red observations.

B. After the thermal jump had occurred;

(1) Micrographs, line scans etc. were taken of the charge-collection signal from the collector-base junction of the 'jumped' device under as wide a range of current and bias conditions as possible compatible with device safety i.e. under conditions such that the thermally-induced changes are reversible.

(2) Devices that had been permanently degraded, either with intent or inadvertently, were examined so that the nature of the damage and its relation to the reversible changes was recorded.

2(b) Infra red microscopy

We used a Barnes infra-red microscope in these studies. The mode of use of this instrument was conventional an ' will not be described here. In the bulk of these initial studies we were only concerned with relative estimates of the temperatures and so were not concerned with calibration troubles arising from uncertainties in surface emissivity. To study the relative thermal behaviour of the 'fingers' the total radiance falling within the collection angle of the microscope was measured as a function of position along each finger under stable conditions. Due care

was taken to stay within the Al strip along each emitter finger.

Subsequently we made measurements on devices which had had a carbon film ($\sim$400Å thick) evaporated onto them. This film did lead to an increase in leakage current flowing through the device under a given bias, but the fractional increase in wattage is small.

3. Experimental results

3(a) Initial search for variations in electrical behaviour along the emitter fingers

We examined the charge collection signal from the collector base junction using the circuit given in figure 1(c). By using relatively high beam currents we were able to detect differences in charge collection behaviour along the various emitter fingers. Figures 2 and 3 show a typical set of observations. The device had been heated by passing an emitter current of .19 amps through it with a collector bias of 26 volts. The device was allowed to cool and micrographs taken as a function of V_{eb} (to give .19 amps) with the emitter and base shorted. As the device cools the very bright, white signal observed in the emitter fingers decays away until the emitter fingers reach a uniform 'grey' against the 'off white' signal from the base area. See figure 2(i) which is typical of the cold device with no emitter current flowing. The main point about the

bright signal from the emitter fingers is that it differs in extent, in position, in persistence from finger to finger and in the temperature at which it becomes apparent as the device is heated. This effect is reversible and occurs at emitter currents well below that at which the thermal jump occurs.

For completeness we have shown (in figure 2(j)) the effect of increasing the emitter current without any associated heating effect. The main effect, compared to the zero current case shown in figure 2(i), is to increase the signal from the emitter region compared to the base area. In this case the signal, although increased, is much more uniform over the emitter area. Only when heating occurs does the signal vary greatly along a given finger and from finger to finger.

It is important to establish whether this temperature sensitive contrast is of importance in thermal runaway problems or whether it has a trivial origin. It is therefore convenient to consider the interpretation of this contrast at this point.

3(b) Initial interpretation of the 'temperature sensitive' contrast

The 'off-white' signal characteristic of the base-collector junction remote from the emitter fingers occurs by the mechanism marked 1 in figure 1(d) i.e. the electrons collected by the collector flow

to earth through the preamplifier and the holes gathered by the base region are neutralised by flow through the base contact. (Process 1 in figure 1(d)). In the absence of an emitter current (figure 2(i)) this process is impeded near the emitter junction probably because the emitter base junction impedes the diffusive flow of electrons to the collector base junction from above. However, when the device is cold but the emitter-base is forward biassed (figure 2(j)) (i.e. an emitter current is flowing) then the holes collected by the base near the emitter can flow to earth by being 'minority carrier injected' across the emitter base junction. (Process 2 in figure 1(d)). The presence of this relatively high conductance path leads to a local increase in the charge collection current. So far the implication is that the base impedance plays an important role. The question arises as to whether it plays a role in the 'temperature sensitive' contrast.

It is thought that the temperature sensitive contrast arises because, as the temperature of a given finger increases, the probability of minority carrier injection at a given location increases so the observed charge collection signal from the base collector junction in that region will increase. All these effects, the temperature dependence, the effect of a self biassed and forward biassed emitter-

base junction - can be summarised in terms of figure 1(e). The self biassed emitter base junction affects the short circuit current, $I_{cco}(z)$ at a given location z. A forward biassed emitter-base junction leads to a large reduction in $R_{eb}(zT)$ and so to an increase in $I_{cc}(z)$. An increase in junction temperature also reduces $R_{eb}(zT)$ and so increases $I_{cc}(z)$.

The relative magnitude of the enhancement of the charge collection signal by minority carrier injection at the emitter junction depends on the magnitude of the base resistance $R_b(zT)$. As the magnitude of the base resistance is considered to be of importance in thermal runaway there is hope that we have here a method of examining the localised aspects of thermal runaway. To confirm this idea we examined the charge collection signal from the emitter base junction under the same bias conditions.

3(c) Confirmatory studies of the above interpretation

Using the circuit shown in figure 1(b) the series shown in figure 3 was obtained. The first micrograph was obtained with zero emitter current and outlines the emitter base junction area. Figure 3(b) was taken with $I_E = 170\mu a$ and apart from being slightly less intense there is no significant change. This decrease in signal from a forward biassed

junction is typical as has been shown by other independent experiments on forward biassed diodes (2). Figure 3(c) however, shows a definite decrease in the signal from the centre of the emitter fingers. This decrease continues with increasing emitter current until, in fact, the signals from the centres of the emitter fingers and from the main emitter centre strip become black or negative. This is just the behaviour predicted on the interpretation given above. Firstly, there is normal charge collection at the unbiassed emitter base junction. At small forward biasses this signal is reduced by minority carrier injection. This mechanicam can result in a diminution of signal but cannot result in a reversal of the signal because the charge collection signal cannot be less than the compensating minority carrier injection. To account for the change of sign we have to consider the behaviour of the adjacent base collector junction. When the emitter is forward biassed the charge collection signal at the collector base junction takes the path through the emitter discussed in section 3(b), and so flows through the preamplifier. As this signal opposes the charge collection signal at the emitter base junction, it first reduces it, then overwhelms it, i.e. leads to a reversal in sign.

It is therefore reasonable to conclude that we have established a means of studying variations in base resistance along the emitter fingers of a multifingered device. This method issimilar tothat already used in surface barrier studies (3). The next problem is how to apply it to the present problem of the 'thermal jumps' observed in this transistor. In order to do this, it is important to establish whether we can relate these variations to temperature differences or not.

4. Initial infra-red microscopy

4(a) Comparison between SEM and IR studies.

We made comparison studies between the SEM studies on a given device and the relative temperature distribution as measured by the IR microscope. In this case the device was examined with its surface untreated i.e. emissivity unchanged. The SEM observations are shown in figure 4(a). It can be seen that the fingers give a variety of behaviour but the two main groups are those which give a near uniform signal along the length of the fingers and those which give a peak signal near the end of the finger. We shall see below that this is an oversimplification but it will suffice for the present. Figure 5(a) and (b) shows relative

temperature measurements made before the SEM studies. We are concerned here with the essentially horizontal parts of these curves. The apparent rapid rise in temperature at the finger ends is probably due to the fact that the emissivity changes from that of the Al strip to that of the oxide. The drop in temperature along the centre 'spline' is probably genuine as the emissivity of the spline is the same as that of the fingers. The probable cause of this drop is the presence of the five substantial Au bonds and the associated thermal conduction and nett increase in surface area. It is not possible to detect any correlation between the charge collection behaviour and the relative temperature studies. Neither the temperature distribution along the fingers nor the average temperature bears any discernable relation to the variations observed in the SEM. The mean temperatures are shown in Table 1. In considering the results shown in figure 5 and Table 1 it should be remembered that the bonds can possibly intercept some of the radiance from some fingers and so can effect the measurements from the right-hand fingers. In general terms we can say from these results that the variations along the fingers are of the order of 12% which is about 3 times the random error and that

Table 1. Measurements of relative temperature of the emitter fingers of the device shown in figure 4.

Finger number	Maximum relative temperature	Minimum relative temperature	Mean relative temperature
29	34	32.5	33.0
27	35.0	34.0	34.5
25	35.0	34.0	34.5
23	36.0	33.5	35.0
21	35.0	34.0	34.5
19	35.0	34.0	34.5
17	32.5	31.5	32.0
16	32.0	29.0	31.0
14	32.5	30.0	31.5
12	34.0	31.0	32.5
10	33.0	29.5	31.5
8	33.5	29.5	31.0
6	34.0	31.0	32.5
4	32.0	30.0	31.0
2	30.5	29.5	30.0

these small variations do not correlate directly with the variations in charge collection. To check further on this absence of correlation

we examined a group of four fingers in more detail. The fingers chosen were 21 to 24. In this group 2 of the fingers gave a low but uniform signal (fingers 21 and 24) and the other two gave a varying signal particularly finger 22. To remove one cause of uncertainty - the fact that the observed changes were only a few times the probable error - we heated the device to a higher temperature and obtained the plots shown in figure 5(c). The shape of the curves are remarkably similar in all four fingers. Only in the maximum temperature is there any indication of the variations seen on the conductive micrographs, in that the most uniform finger has the lowest temperature of the four, while the finger with the most variation in signal has marginally the highest temperature. In fact the maximum temperature correlates with the variation in charge collection signal for all four fingers, but the variations in maximum temperature are small. To attempt to put some figures to this correlation we obtained line scans along the fingers. Some of these line scans are shown in figure 6. If we plot the maximum fractional variation in I_{cc} against maximum temperature we obtain the results in table 2. As the variation in maximum temperature is of the order of

Table 2. Maximum temperature against fractional change in I_{cc}

Finger	$\Delta I/I_{max}$	max" temp. "(a)	max"temp. "(b)
21	.26	49.5	63
22	.425	50.5	62.5
23	.40	50.0	63
24	.164	47.5	61

the experimental uncertainty we repeated the relative temperature measurements at a higher temperature (see final column in table 2). It is apparent that the correlation needs further substantiation if it is to be upheld. The position is best summarised by saying that where there are significant temperature differences (between finger 24 and the others) the variation in charge collection signal is less in the cooler finger. When the temperature changes between fingers are not sufficient to be detected there are still significant variations in charge collection signal. Leaving aside the detailed cause of these variations, it appears that the model necessary to explain these observations can be stated as follows:-

up to the power levels studied so far the temperature variations in the fingers is small. (There is a slight increase in temperature towards the centre of the device. See fingers 23 and 12). Where there are small but significant differences in temperature the cooler fingers give a weaker but more uniform signal than the hotter fingers in agreement with the ideas discussed in section 3(b). We shall return to this topic in section 5(b) where we consider the behaviour in the 'jumped' condition. First it is convenient to consider the possible role played by mechanical defects in causing these variations between the fingers.

4(b) Effect of mechanical defects

The charge collection signals from the collector-base junction and the emitter-base junction were examined under a wide range of conditions without sufficient power dissipation to cause significant junction heating. The only mechanical defects found are illustrated in figure 4. In figures 4(d) and (e) it is apparent that the signal from the emitter fingers and from the central spline indicates a distribution of linear regions of reduced signal having a three fold symmetry. This signal distribution indicates the presence of diffusion induced slip (4)

owing to the lattice misfit arising from the use of high doping levels. We examined over twenty fingers on three devices to establish whether variations, either in density or distribution, of this diffusion induced slip could be related to variations in the temperature sensitive contrast observed in the emitter fingers. It was found that the distribution of diffusion induced slip was remarkably uniform and that the variations in the temperature sensitive signal from the emitter fingers could in no way be related to variations in the slip pattern., Since this was the only type of microscopic defect observed it was reasonable to conclude that the underlying cause of the observed contrast is related to variations in degree of some property such as doping level, bulk resistivity etc. rather than the presence of some localised defect.

To sum up the data obtained in the 'pre-jump' mode:- There are temperature sensitive contrast variations observed in the emitter fingers. These variations are probably associated with variations in base resistance. It is possible that the observed variations are due, in part, to variations in temperature but further

work is needed to substantiate this claim. For the present it is more important to see if we can establish any contrast features associated with the thermal jump.

5. Direct observation of a reversible thermal jump

5(a) General

The method of examination consisted of

(a) mounting the specimen device on a suitable heat-sink and examining the electrical behaviour in air as the emitter current was increased until the jump had occurred.

(b) Once a clear idea of the jump (- the current at which it occurs, its magnitude and the stability of the device after the jump -) had been obtained in air the procedure was repeated in the more heat constricting environment of the SEM vacuum chamber using a water cooled heat sink to reduce the case temperature.

(c) Subsequently conductive micrographs were taken of the device at low currents, and at high currents just before the jump occurred.

(d) Finally contrast features associated with the jump were sought.

5(b) Contrast due to reversible thermal jumps

Consider the observations shown in figure 7. The device chosen was a particularly uniform one from the viewpoint of the nearly identical contrast observed in the emitter fingers. This uniformity can be seen from figure 7(a) which is a charge collection 'map' taken of the collector-base junction with a small emitter current flowing through the device. As the emitter current is increased the observed signal drops, the enhancement of signal at the ends of the emitter fingers decays and signal from the whole of the emitter finger area becomes increasingly uniform. This situation persists until the jump occurs at which point a region, usually including several fingers, will suddenly give a reduced signal. Figure 7(b) shows such a region for the device being considered. These regions often occur near to the centre spline and away from the finger ends. A close examination of this region of darker signal shows that the main change compared to the signal before the jump is that the signal from under the emitter fingers is reduced. The shape of these darkened areas is often an elongated circle or ellipse. In the case illustrated in figure 7 the dark region extends further down the side of the centre spline as the emitter current is increased. This elongation can be seen in figures

7(b) and (f) which were obtained at constant collector-base voltage. On the other hand, if the emitter current is kept constant and the collector base voltage is increased, the area of darkened signal does not increase in extent as can be seen from figure 8. In this case the increasing power density appears to be dissipated through a constant area and so, eventually, the device runs away.

It is obviously necessary to confirm whether the darkened region observed when the jump occurs is associated with a temperature change or not. In order to do this we made relative measurements of the surface temperature of the device shown in figures 7 and 8 in both the non jumped and in the jumped condition. These observations consisted of making measurements of the emitted radiance from various points on the emitter fingers. Care was taken to keep the optical system imaged on the emitter metallising. In this way, although the emissivity was unknown, it was constant throughout the measurements. These measurements are shown in figure 9. Figure 9(a) represents a drawing of the

emitter area. The number at a given location represents the radiance from that area after the jump had occurred. It is apparent that the region of darkened signal in figures 7(b) to (i) does correspond to the incipient runaway region or hot spot. The data plotted in figure 9(b) represents the observed radiance plotted as a function of position along the hottest finger (that marked AB, in figure 9(a)). The curve outlined by the square data points is indicative of the general level of the fingers in this area prior to the jump. The estimates of temperature made prior to the jump were insufficiently accurate to tell whether there was a temperature gradient along the specimen or not prior to the thermal jump. We therefore have little or no indication as to why the jump occurred in the region it did. The only pertinent comment we can make about the site of failure of this device is to note that it did not fail at the hottest finger. The hottest finger was number three whereas the damaged area occurred in finger 2 and above (see figure 8). Therefore observations of damaged areas do not always give direct indications of the site of the initial cause of failure.

One other observation was made. It is not apparent from figures 7 and 8 whether the signal continues to decrease as the wattage is increased, as the signal in the relevant area is small and changes are difficult to detect. Further studies, however showed that as the darkened area extends the signal reaches a minimum near to the centre of the initial area and that this minimum gets lower as the power is increased. The implication is that the darkening (or drop in signal) increases monotonically as the temperature increases.

Although the above results establish that it is possible to observe reversible hot spots under non avalanching conditions several questions remain. Particularly important is an understanding of why the hot spot occurs in the area it does. To seek an answer to this question we made the radiance plots shown in figure 10. The data in figure 10(a) were obtained before the thermal jump occurred. Whereas the observations in figure 10(b) were obtained after. The heavy number in the circle corresponds to the finger number shown in figure 12. Figure 12 shows charge collection micrographs of the device before and after the thermal jump has occurred. (Note figure 12 is printed in a mirror image relationship compared to figures 10 and 11). The

small numbers in figure 10 indicate the radiance at the particular point. Figure 11 shows the contour maps obtained by inspection from these data. Two features are apparent. One point is that there is a substantial temperature variation prior to the thermal jump and that this variation occurs over a region which is large compared to the individual fingers. The second point is that the temperature maximum after the jump has occurred does not coincide with the region of highest temperature prior to the jump. Obviously with only one set of observations it is premature to draw conclusions, but the result is significant in that the differences cannot be accounted for in terms of experimental error.

5(c) Physical mechanism whereby thermal jumps are observed

It is important to establish what physical parameter is being used to observe the local hot spots. To determine this we initiated a series of measurements of the temperature dependence of the charge collection signal first from an isolated junction, i.e. a junction separated from other junctions by a sufficient distance to avoid all coupling action. The initial measurements are shown in figure 13.

These were obtained from a planar guard-ring diode having a breakdown voltage of ~22V. The device was heated up uniformly in the SEM by means of a special heating stage, the temperature being monitored by means of a thermocouple located close to the TO5 header on which the device was mounted. It is apparent that for an isolated p-n junction, at bias voltages up to $\sim \frac{1}{2}$ of the breakdown voltage, the charge collection signal tends to increase with temperature up to $\sim 200^{o}C$ and then to decrease.

In the experiments reported here, the power transistors were operated with V_{CB} = 25 40V, this junction having a breakdown voltage in excess of 100V. No evidence of the signal level from the collector base junction increasing with device temperature was observed. Thus it appears that the mechanism which leads to the SEM observation of hot spots in transistors under normal operating conditions depends on the presence of the forward biased emitter base junction. In order to enquire further into this mechanism, a hot stage is being constructed for the SEM which will enable a TO3 header to be heated uniformly from an external supply while the device is being operated at low bias values. In this way, the effect of temperature on the interaction between

the two junctions can be studied.

5(d) Conclusions on the observation of thermal jumps

The IR microscopy measurements confirm that the contrast changes seen in the SEM when the power dissipated in the transistor reaches a critical level are associated with a reversible thermal jump. The indications are that the drop in signal seen at the hot spot is a measure of the temperature distribution, but exact correlation has not been confirmed, and may necessitate mounting the IR microscope on the side of the SEM so that simultaneous observations can be made.

The exact mechanism which gives rise to the observed contrast at the hot spot is not fully understood, and further experiments are under way to elucidate this. Preliminary results indicate that it is a function of the proximity of the emitter base junction to the collector base junction.

6. General conclusions

The application of the SEM to the study of thermal effects in power transistors has resulted in two new forms of contrast in the conductive mode. The first is seen at low power dissipation and is associated with the microscopic variations in the base resistance under the emitter fingers. The second form of contrast is seen at higher power levels when the device

performs a reversible thermal jump, and is associated with the formation of a hot spot as confirmed by IR observations.

The extent of these hot spots has been studied as a function of the power dissipated in the device, and is shown to differ depending whether the emitter current or the collector base voltage is increased to increase the power dissipation. The cause of the hot spot, i.e. why one particular region forms a hot spot as opposed to an apparently identical adjacent region, is not immediately apparent from the IR or the low power SEM studies, and further work on this will include a systematic study of a number of devices to establish a statistical relationship between the various results obtained.

Acknowledgements

The authors would like to acknowledge the support for this work obtained from the Ministry of Defence (Navy Department) and the National Aeronautics and Space Administration. Also to S. T. C., Footscray for supplying the experimental devices.

References

1. C. Millward, K.A. Hughes and P.R. Thornton, Annual Report, August 1966 to December 1967 on C.V.D. Contract CP3632/66.

2. D.V. Sulway, Ph.D. Thesis, U.C.N.W. Bangor (1968).

3. I.G. Davies, Ph.D. Thesis, U.C.N.W. Bangor (1969).

4. W. Czaja and J.R. Patel, J. Appl. Phys., 36, 1476, (1965).

Captions to Figures

Figure 1 (a) Schematic outline of transistor illustrating emitter fingers.

(b) Circuit used to obtain charge collection signal from the emitter base junction.

(c) Circuit used to obtain charge collection signal from the collector base junction.

(d) Illustrates the competing paths for holes created by the beam in the base region of the device (for details see text.)

(e) The equivalent circuit used to illustrate the factors on which the charge collection signal depends (for details see text).

Figure 2 Charge collection micrographs obtained from the collector base junction (fig. 1(c)) as the transistor cools down after being heated by a current of 0.19A at V_{CB} = 26V. The mean temperature for each micrograph was estimated by momentarily applying an emitter current and measuring V_{EB} before and after each micrograph was

taken. V_{EB} at room temperature was assumed to be 677mV and $\Delta V_{EB} = 2.3\text{mV}/^{o}\text{C}$. The values so obtained were:

(a) $V_{EB} = 405\text{mV}$, $T = 418^{o}\text{K}$ (b) $V_{EB} = 425\text{mV}$, $T = 410^{o}\text{K}$ (c) $V_{EB} = 438\text{mV}$, $T = 404^{o}\text{K}$

(d) $V_{EB} = 450\text{mV}$, $T = 399^{o}\text{K}$ (e) $V_{EB} = 469\text{mV}$, $T = 391^{o}\text{K}$ (f) $V_{EB} = 476\text{mV}$, $T = 387^{o}\text{K}$

(g) $V_{EB} = 496\text{mV}$, $T = 379^{o}\text{K}$ (h) $V_{EB} = 506\text{mV}$, $T = 375^{o}\text{K}$ (i) $V_{EB} = 523\text{mV}$, $T = 367^{o}\text{K}$

(j) shows how a similar white signal is brought up by passing current through the device; $V_{EB} = 460\text{mV}$, $T = 395^{o}\text{K}$.

Figure 3 Charge collection signal obtained from the emitter base junction, (fig. 1(b));

(a) With $I_E = 0$, (b) $I_E = 107\mu\text{A}$, (c) $I_E = 200\mu\text{A}$, (d) $I_E = 830\mu\text{A}$, (e) $I_E = 4\text{mA}$.

Figure 4 (a) Conductive signal obtained from the collector base junction of the transistor as the device is cooling down with $V_{CB} = 20\text{V}$, $I_E = 0\text{ma}$, $V_{EB} = 341 \rightarrow 401\text{mV}$. For convenience, the emitter fingers were numbered from 1 to 32, 1 to 16 being on the right of this micrograph starting at the top, and 17 to 32 being on the

left starting from the bottom.

(b) Higher magnification micrograph of the device obtained under similar conditions as (a). Fingers 21 to 24 are arrowed, the lowest being number 21.

(c) Conductive signal obtained from the collector base junction with I_E = 130ma, V_{EB} = .425V, V_{CB} = 18.4V.

(d) Signal from emitter base junction with I_E = 0 showing the defects observed. The arrows emphasise the direction of these.

(e) Higher magnification of part of (d).

Figure 5 (a) Relative temperature measurements made by IR microscopy along the fingers of the device shown in figure (4). The numbers in the circles refer to the emitter fingers.

(b) as (a) but on the right-hand side of the device. The greater variation is possibly due to the emitterwires intercepting some of the radiation.

(c) IR measurements of fingers 21 to 24 (compare figure 4(b)) with the device dissipating greater power.

Figure 6 Quantitative measurements of the information contained in the micrograph of figure 4(a), along the centre of the fingers of the left-hand side of the device.

Figure 7 Charge collection signal from the collector base junction as I_E is increased.

(a) shows the low power case with I_E = 1ma, V_{EB} = .460V, V_{CB} = 35V.

(b) - (f) micrographs of the device in the 'jumped' condition as I_E is increased.

(b) I_E = .56A, V_{CB} = 29V, V_{EB} = .545 - .496V.

(c) I_E = .7A, V_{CB} = 28V, V_{EB} = .545 - .480V.

(d) I_E = .8A, V_{CB} = 27V, V_{EB} = .545 - .480V.

(e) I_E = .95 - .98A, V_{CB} = 25V, V_{EB} = .545 - .475V.

(f) I_E = 1.05 - 1.1A, V_{CB} = 25V, V_{EB} = .55 - .47V.

Figure 8 (a) - (c) Charge collection signals from the collector-base junction with I_E = 0.56A and V_{CB} increasing.

(d) and (e). Charge-collection micrographs showing this same device after it had been irreversibly damaged by increasing V_{CB}.

(f) Emissive micrograph of part of the damaged region showing where the Al contact has melted.

Figure 9 IR measurements of the temperature distribution on the device shown in figures 7 and 8.

(a) Radiance measurements at locations along the emitter metallising with the device in the 'jumped' condition, $I_E = 0.56A$, $V_{CB} = 30V$.

(b) Radiance measurements along ABCD in (a) - fingers 30 and 3. The values indicated by squares represents the radiance signal obtained just before the jump, with $I_E = 0.53A$.

Figure 10 Radiance measurements on selected fingers of a device.

(a) Immediately before the jump.

(b) Immediately after the jump had occurred.

Figure 11 Radiance measurements on various fingers of a device.

(a) Before the jump has occurred.

(b) After the thermal jump.

Figure 12 Charge collection maps of the device shown in figure 11.

(a) Just before the jump occurs, $I_E = 0.71A$, $V_{CB} = 30V$, $V_{EB} = .675 - .66V$.

(b) Just after the jump occurs, $I_E = 0.71A$, $V_{CB} = 30V$, $V_{EB} = .7 - .685V$.

(c) Increasing emitter current, $I_E = 0.75A$, $V_{CB} = 29.5V$, $V_{EB} = .72 - .705V$.

(d) Device allowed to warm up slightly, $I_E = 0.75A$, $V_{CB} = 29.5V$, $V_{EB} = .69 - .675V$.

(e) $I_E = 0.8A$, $V_{CB} = 29V$, $V_{EB} = .69 - .68V$.

(f) $I_E = 0.85A$, $V_{CB} = 28.5V$, $V_{EB} = .69 - .68V$.

(g) $I_E = 0.9A$, $V_{CB} = 28V$, $V_{EB} = .69 - .68V$.

Figure 13 Graph of the average charge-collection signal across a guard-ring diode junction as a function of temperature for various values of reverse bias. Device breakdown voltage = 22V.

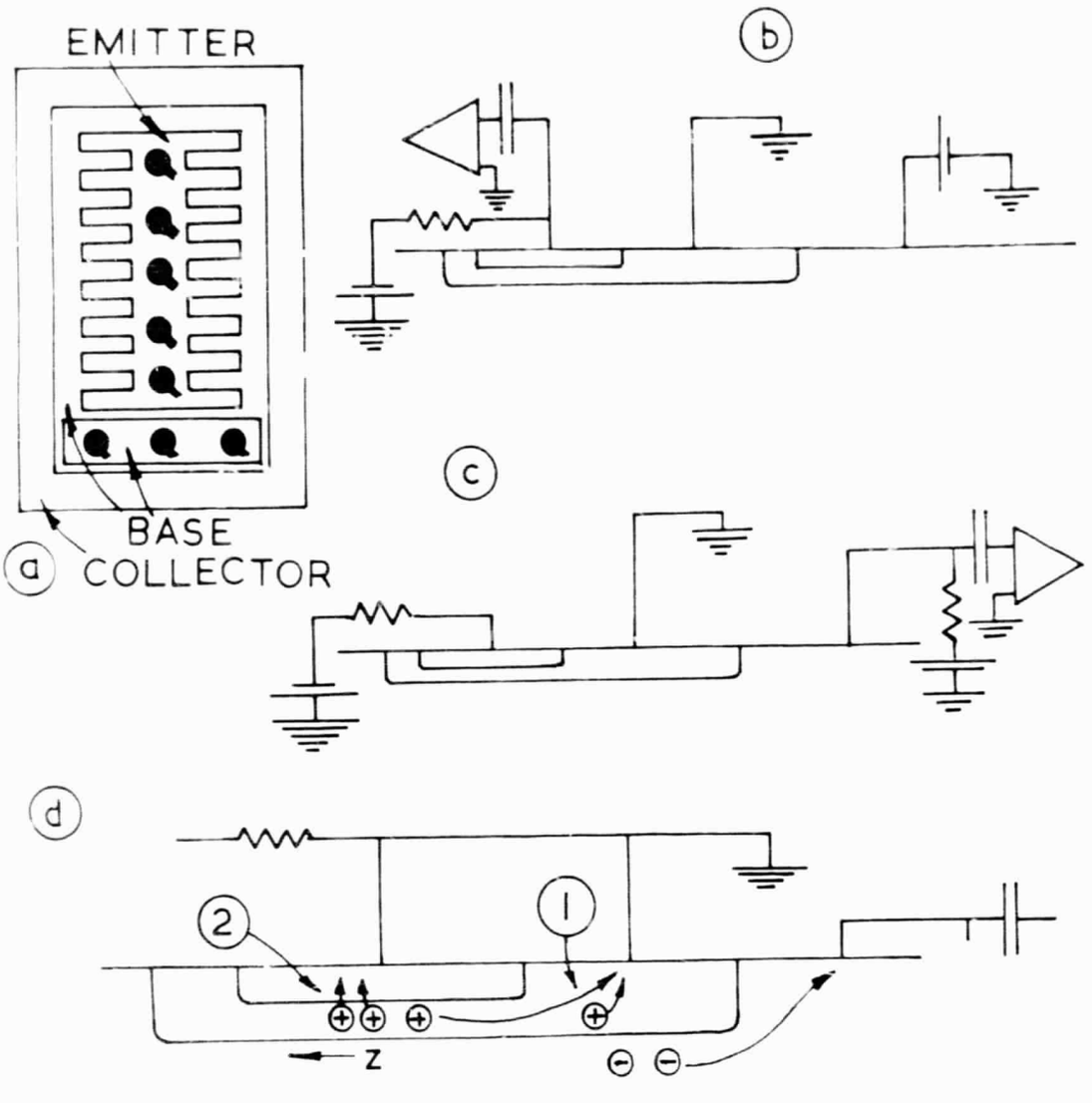
EMITTER
BASE
COLLECTOR
a
b
c
d
2
1
z
e
R_s
$I_{cco}(z)$
$R_{eb}(z,T)$
$R_b(z,T)$
SIGNAL
R_L
$I_{cc}(z)$

FIGURE.1.

FIGURE.2.

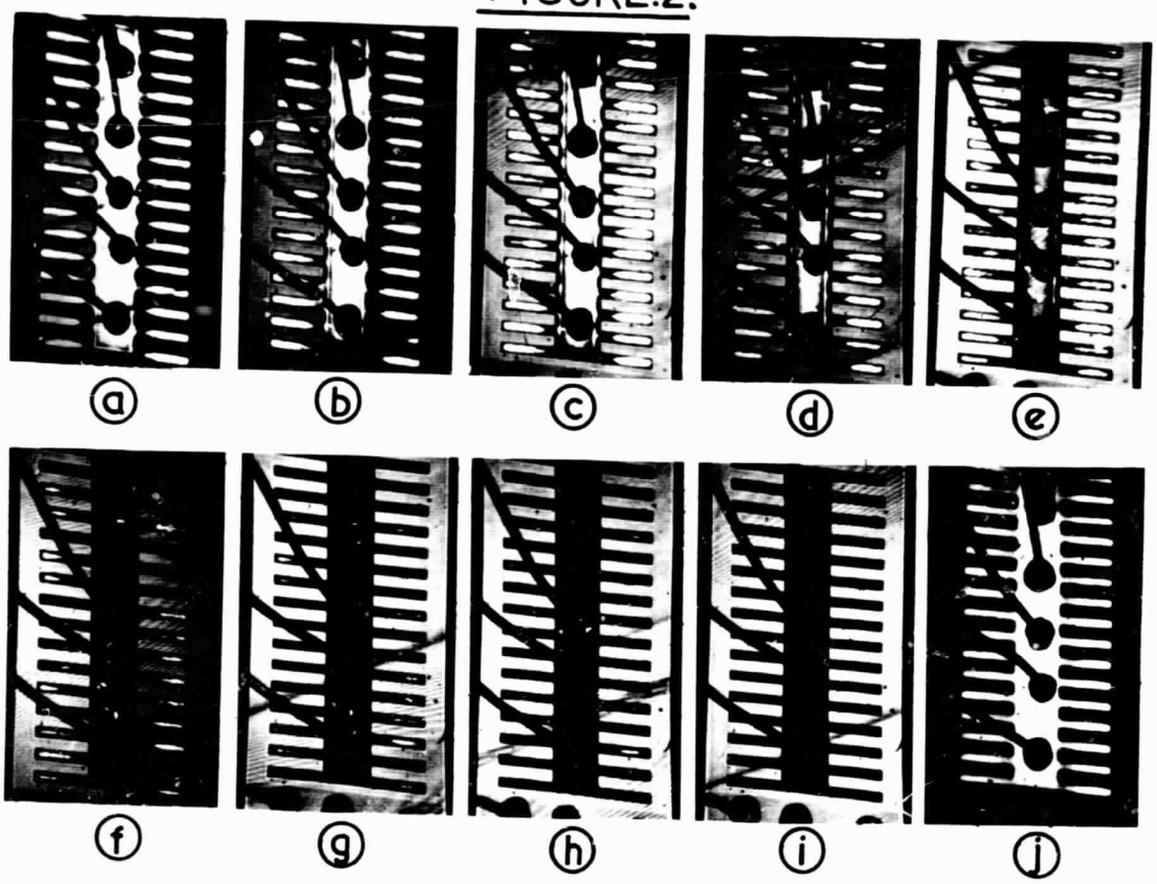

FIGURE.3.

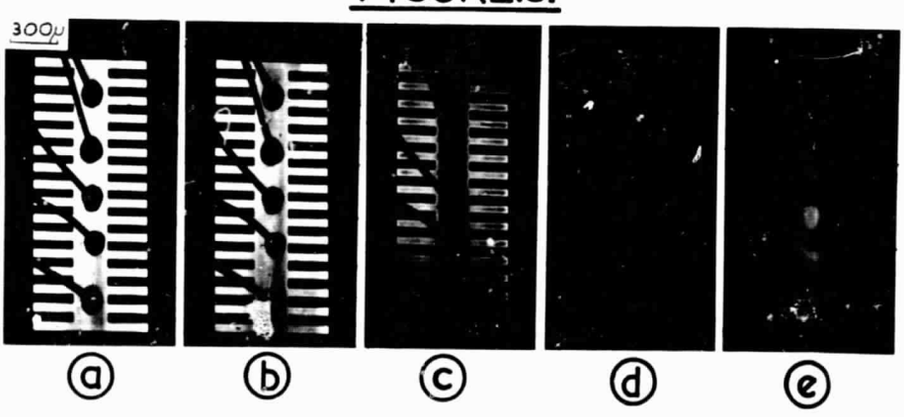

FIGURE.4.

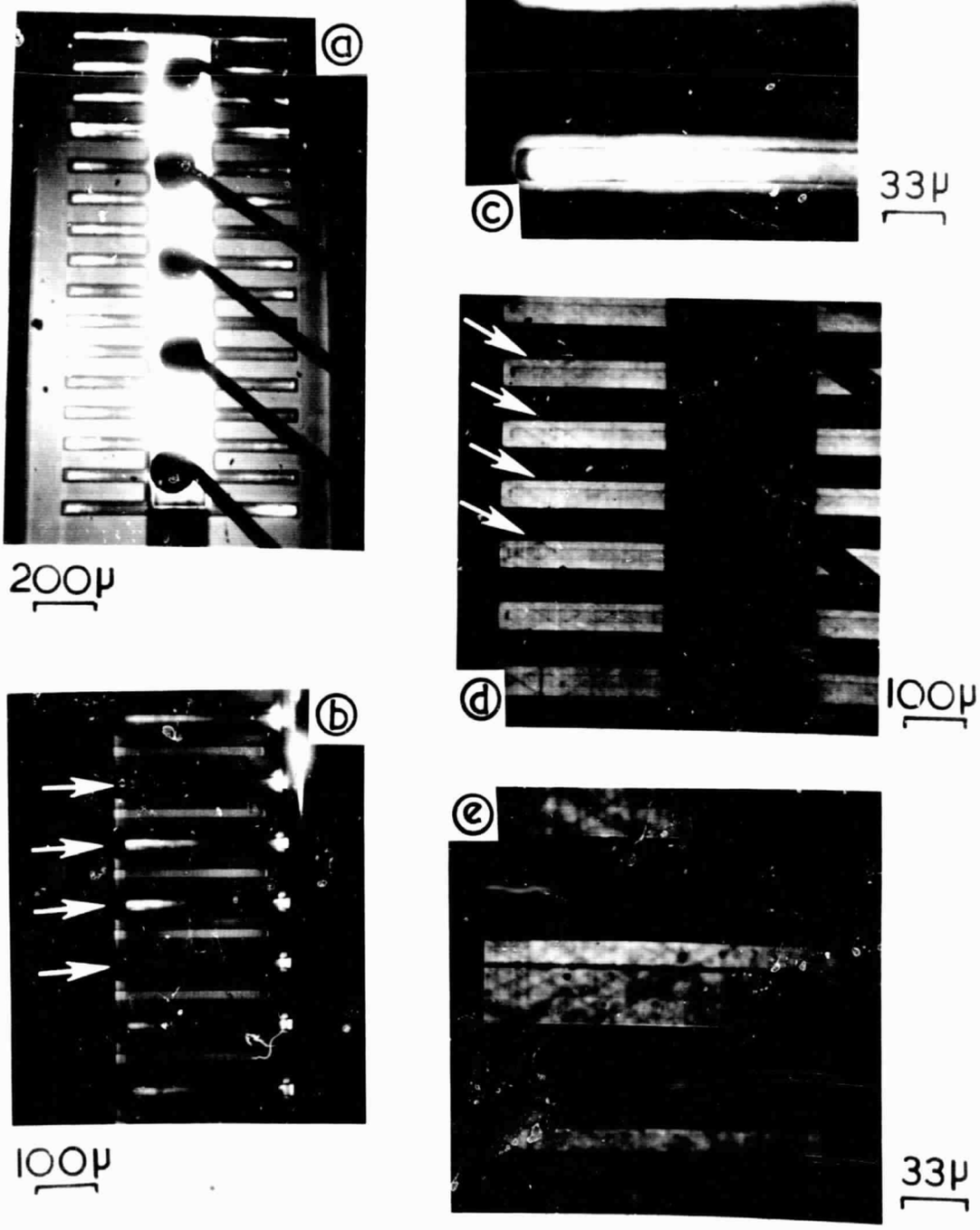

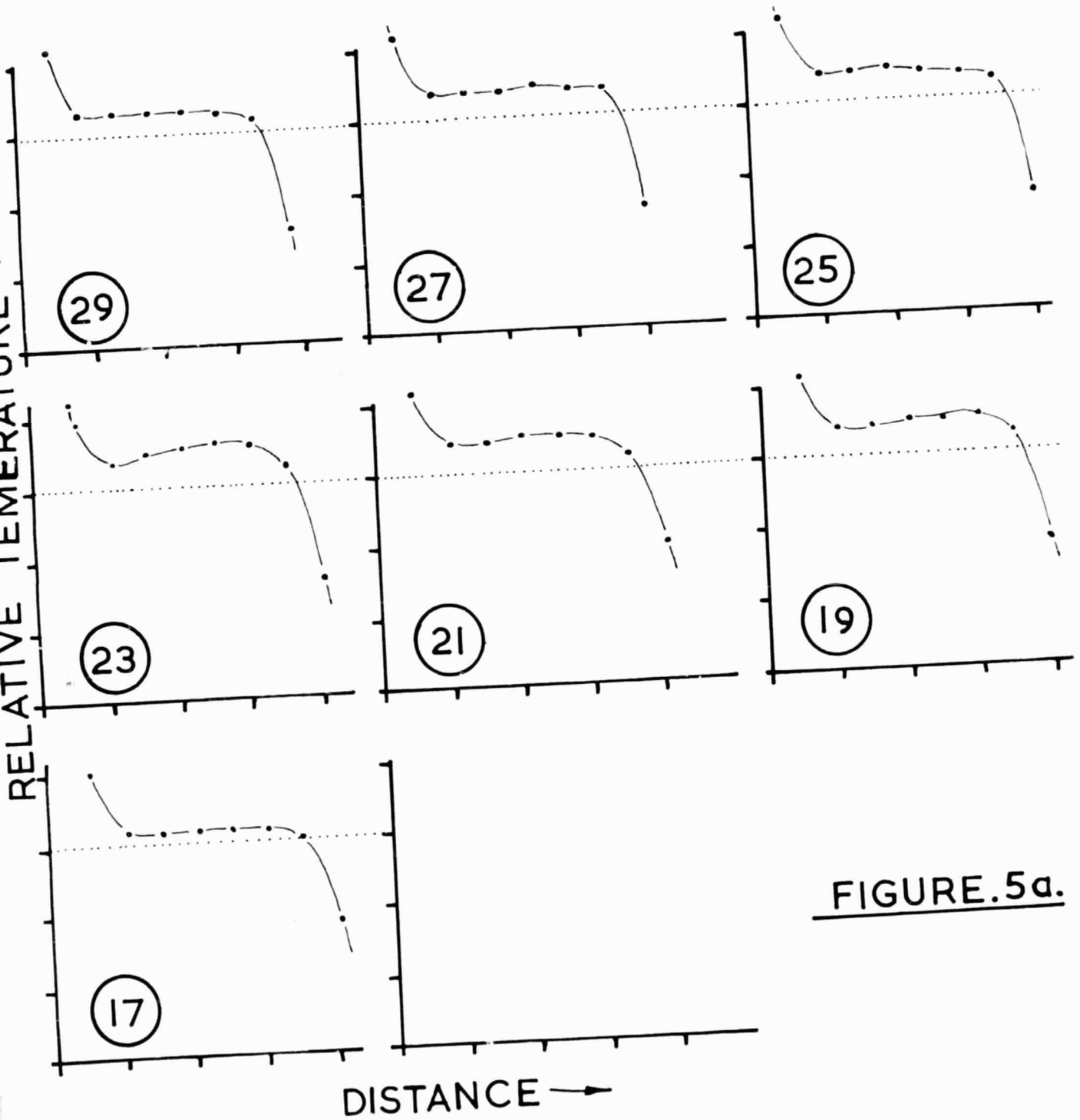

FIGURE.5a.

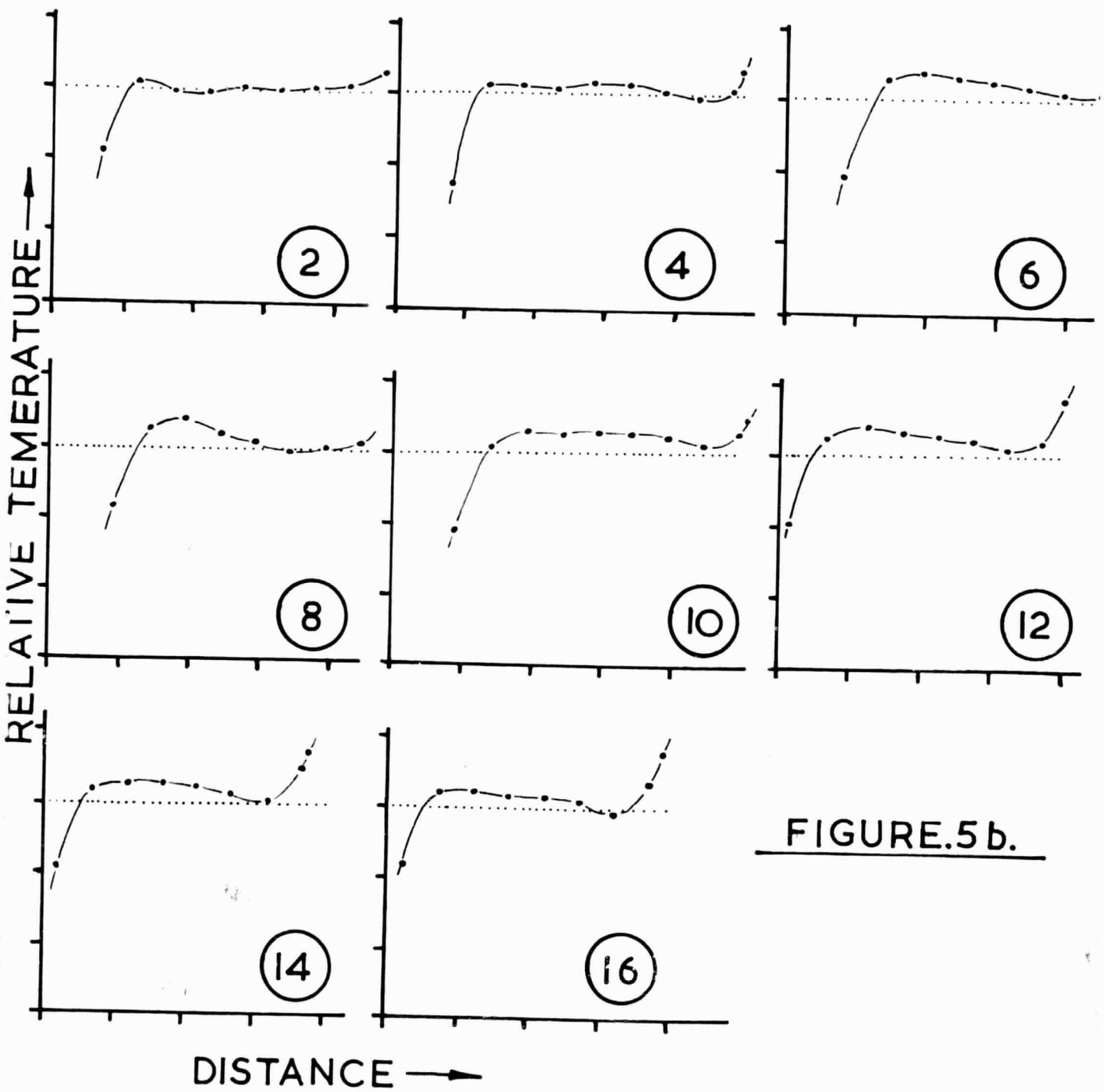

FIGURE.5b.

FIGURE.5c.

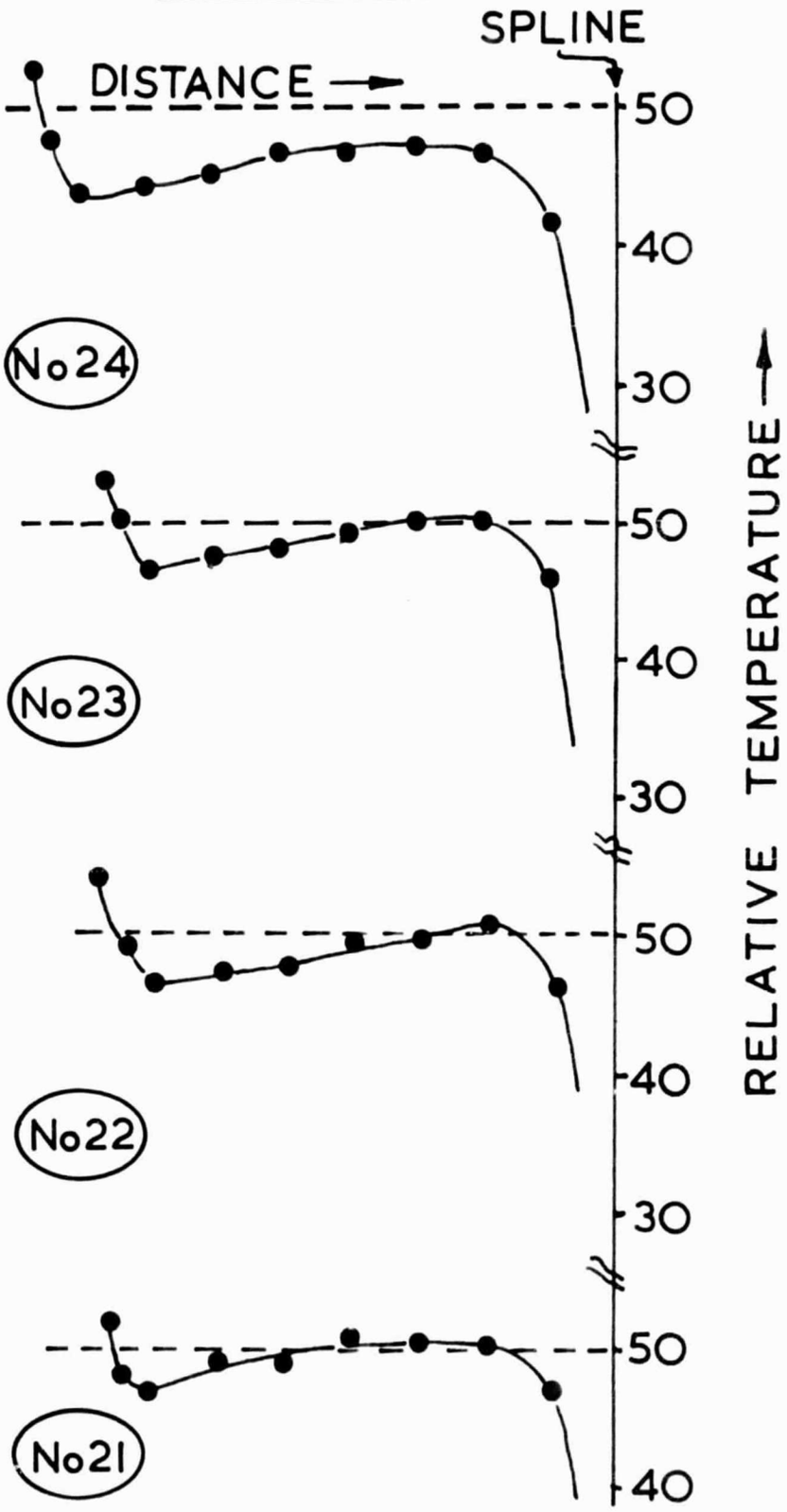
SPLINE
DISTANCE
50
40
30
No24
50
40
No23
30
50
40
No22
30
50
40
No21
RELATIVE TEMPERATURE

FIGURE.6.

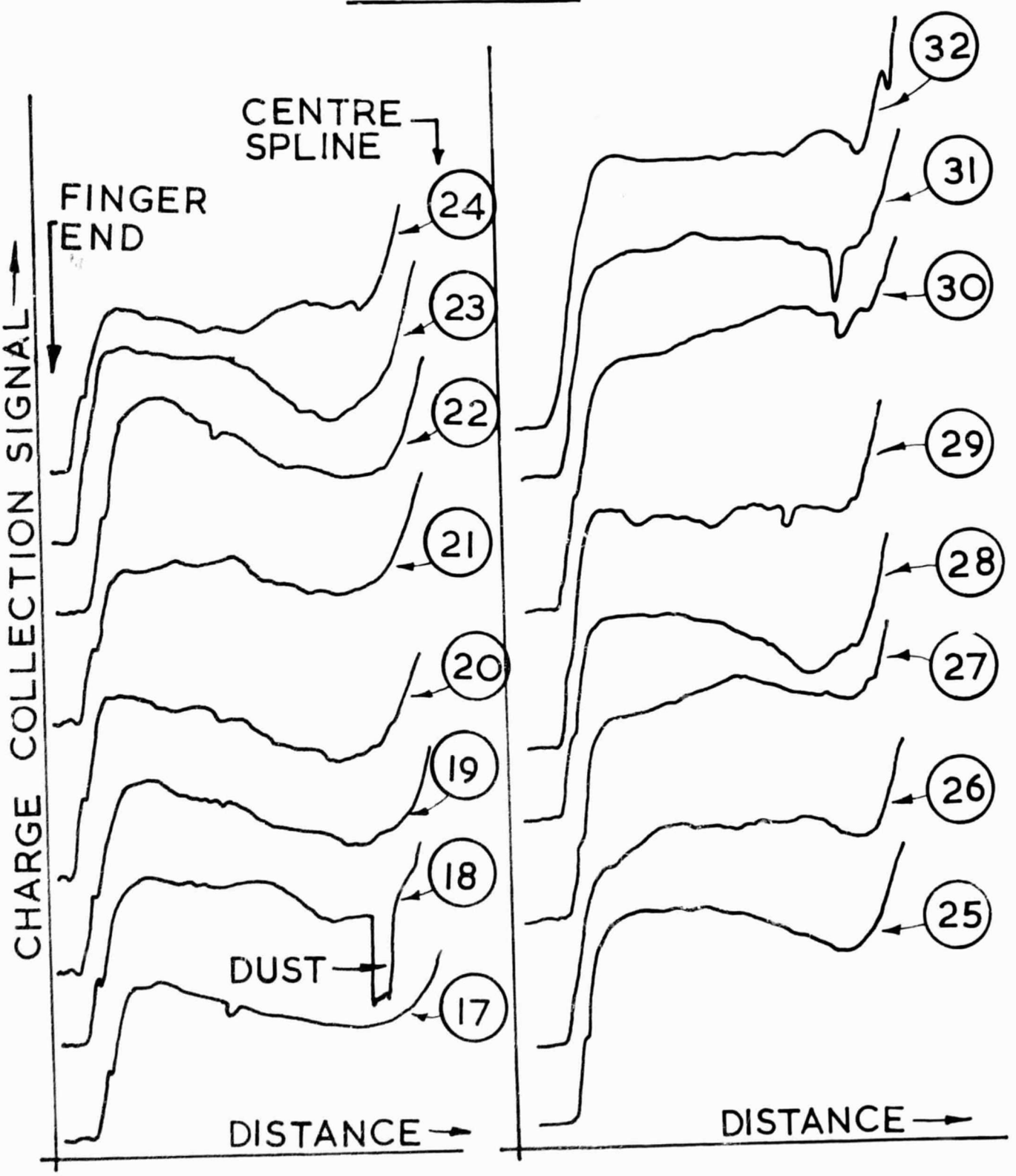
CENTRE SPLINE
FINGER END
CHARGE COLLECTION SIGNAL
24
23
22
21
20
19
18
17
DUST
DISTANCE
32
31
30
29
28
27
26
25
DISTANCE

FIGURE 7

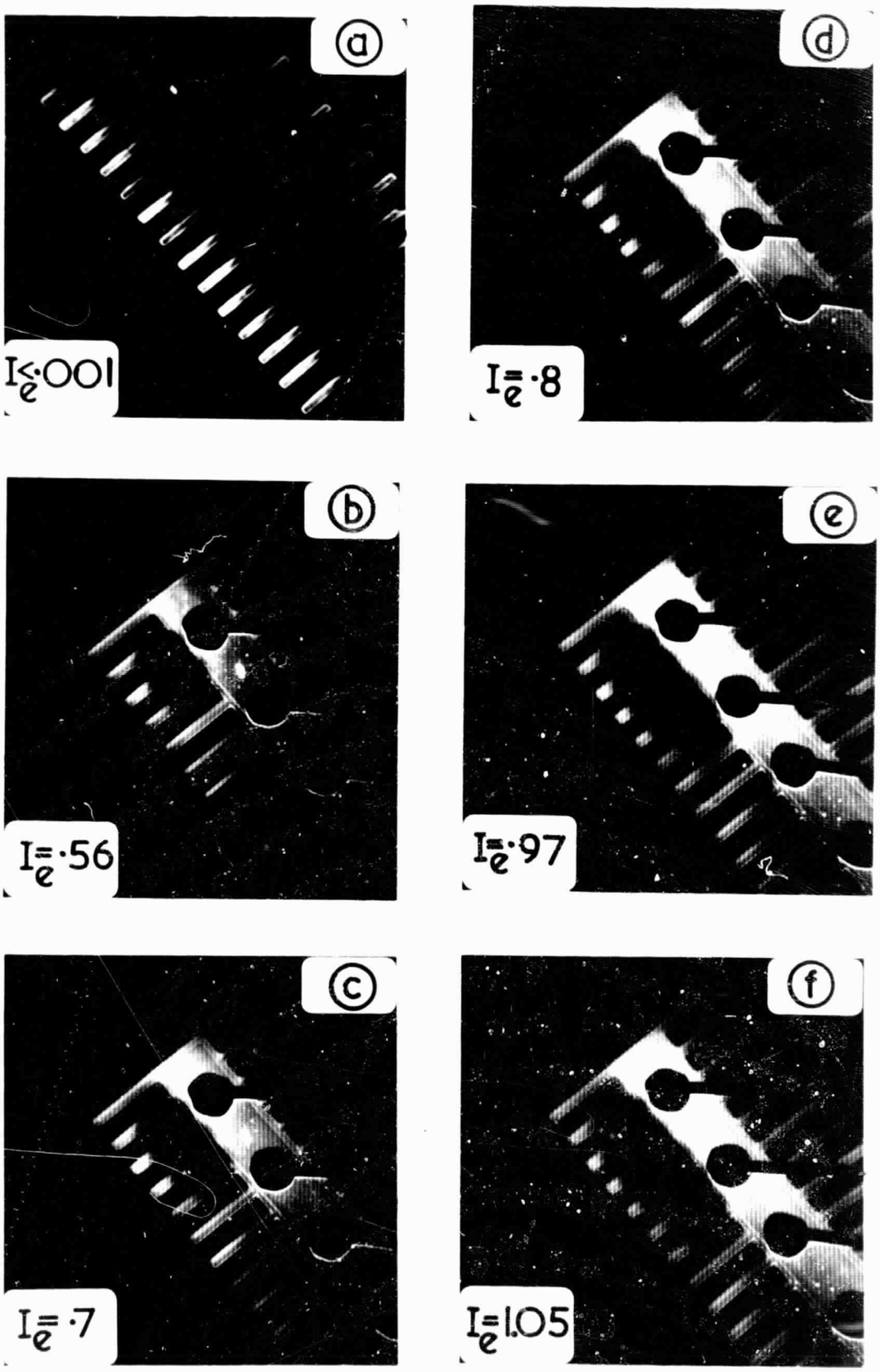

FIGURE 8

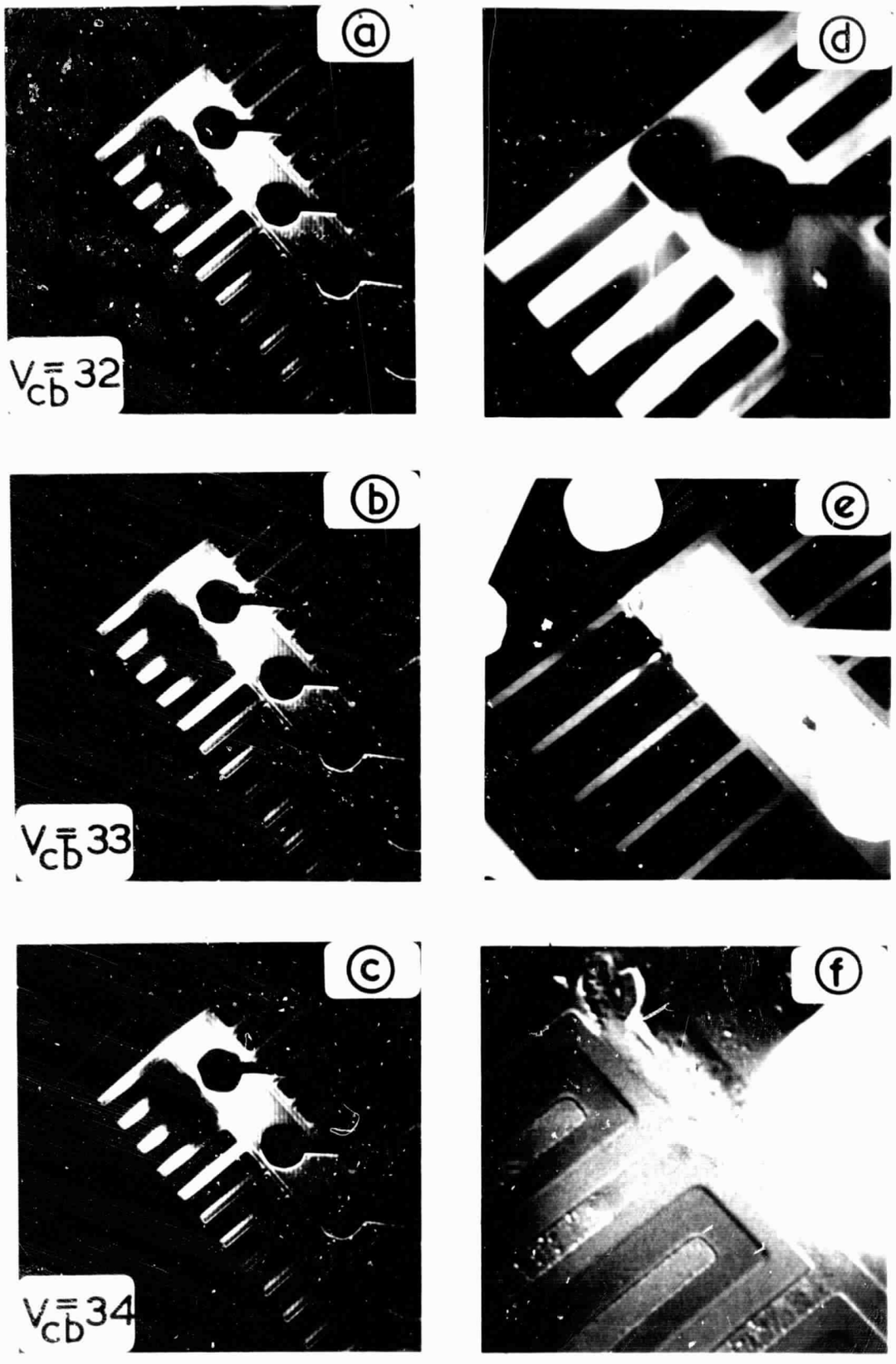

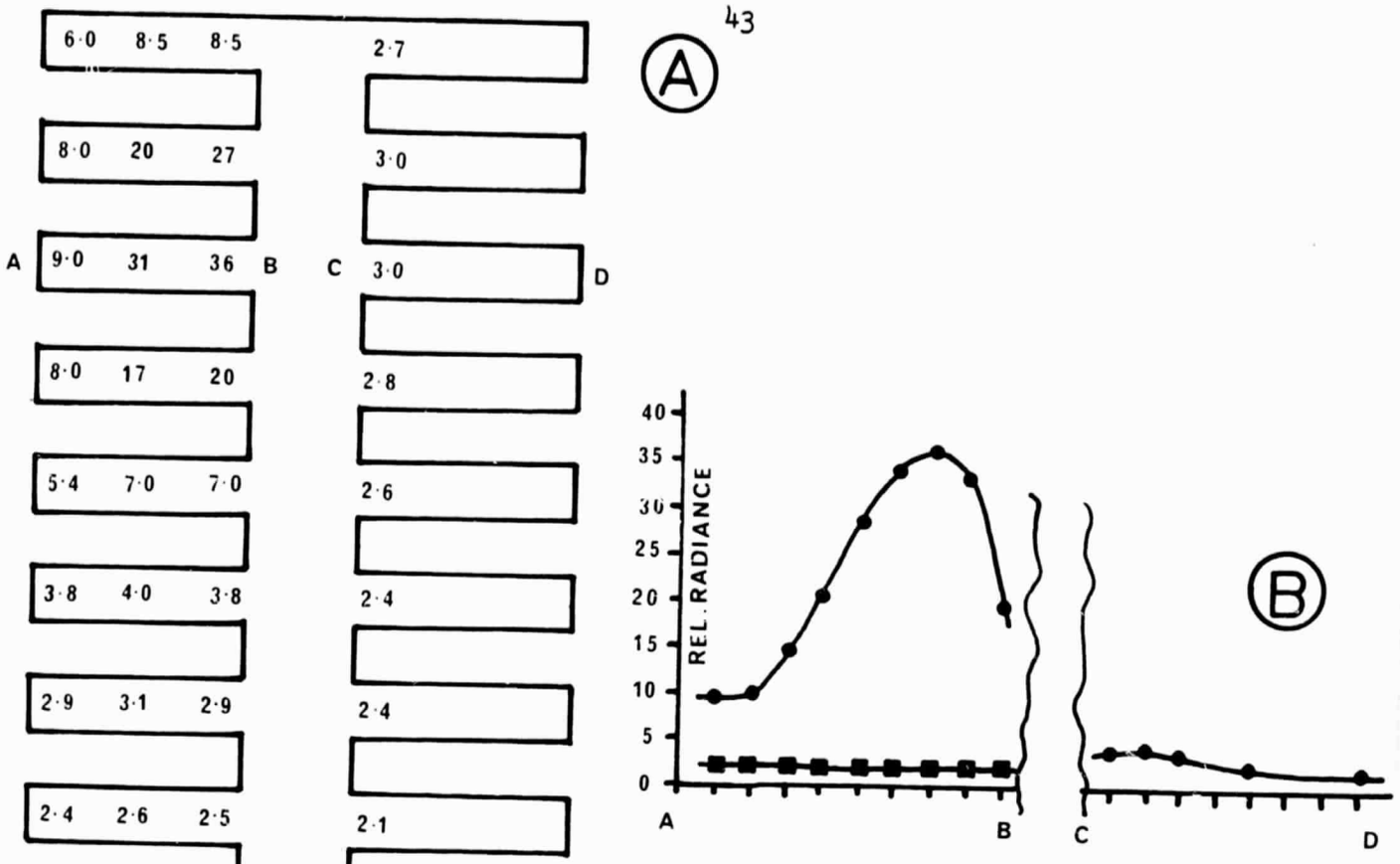
A
6·0 8·5 8·5
8·0 20 27
A 9·0 31 36 B
8·0 17 20
5·4 7·0 7·0
3·8 4·0 3·8
2·9 3·1 2·9
2·4 2·6 2·5
2·3 2·3 2·3
2·2 2·2 2·1
2·0 2·1 2·0
1·9 2·0 1·9
1·9 1·9 1·9
1·9 1·9
1·9 1·9
1·8 1·8
C 2·7
3·0
3·0 D
2·8
2·6
2·4
2·4
2·1
2·0
2·0
1·9
1·9
1·9
1·8
1·8
1·8
B
REL. RADIANCE
40
35
30
25
20
15
10
5
0
A
B
C
D

FIGURE.9.

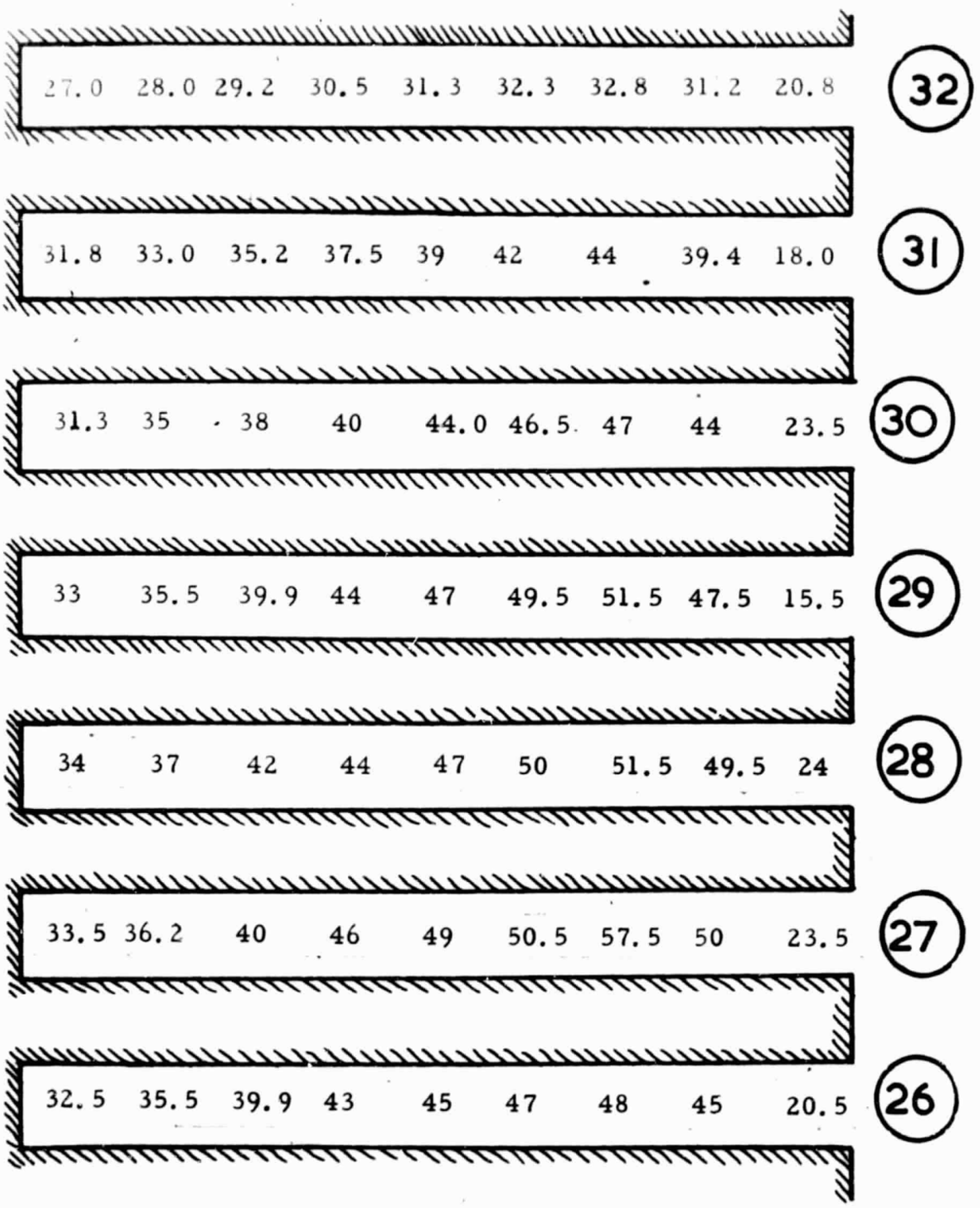
27.0 28.0 29.2 30.5 31.3 32.3 32.8 31.2 20.8
32
31.8 33.0 35.2 37.5 39 42 44 39.4 18.0
31
31.3 35 38 40 44.0 46.5 47 44 23.5
30
33 35.5 39.9 44 47 49.5 51.5 47.5 15.5
29
34 37 42 44 47 50 51.5 49.5 24
28
33.5 36.2 40 46 49 50.5 57.5 50 23.5
27
32.5 35.5 39.9 43 45 47 48 45 20.5
26

FIGURE 10.a.

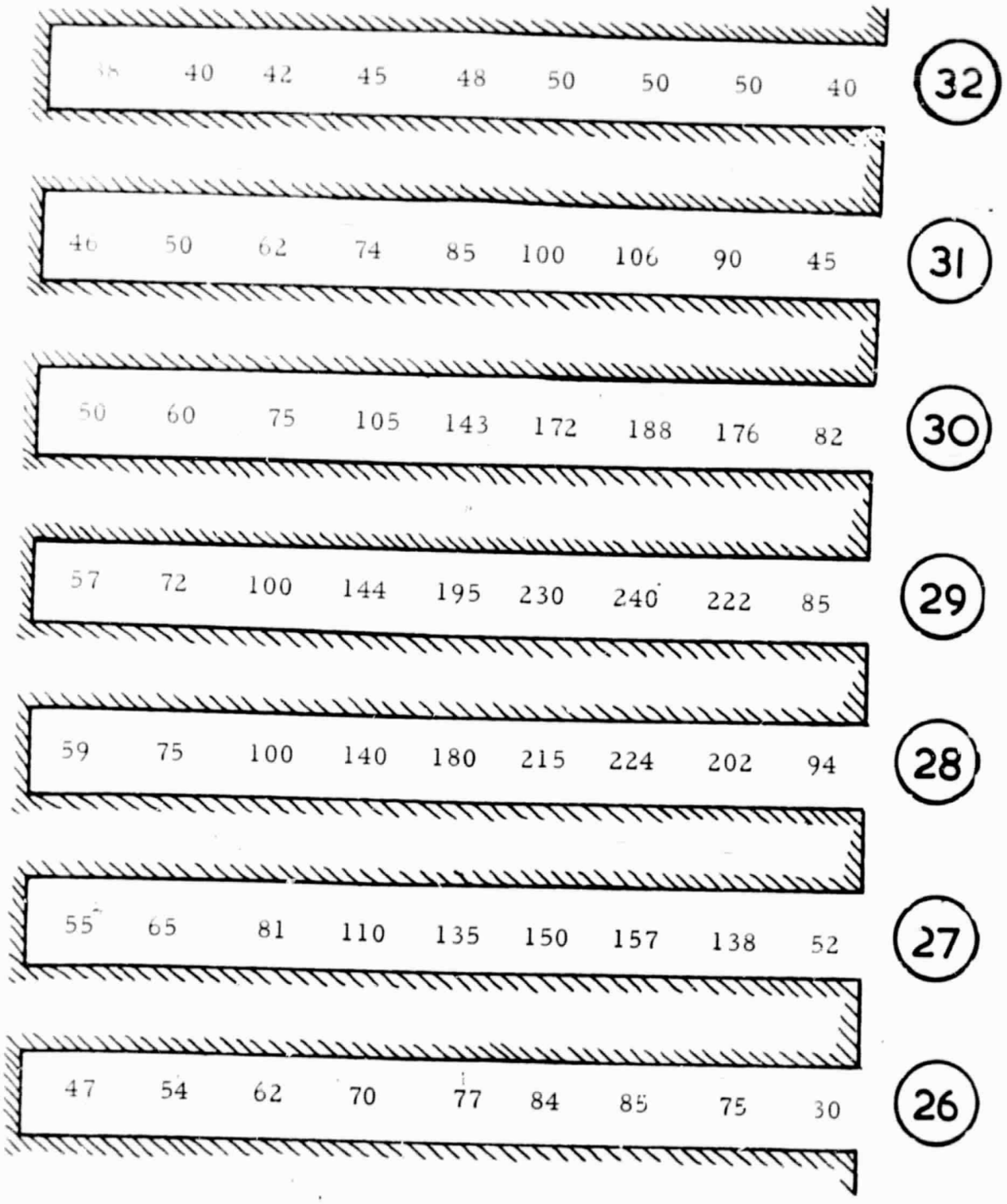
38 40 42 45 48 50 50 50 40
32
46 50 62 74 85 100 106 90 45
31
50 60 75 105 143 172 188 176 82
30
57 72 100 144 195 230 240 222 85
29
59 75 100 140 180 215 224 202 94
28
55 65 81 110 135 150 157 138 52
27
47 54 62 70 77 84 85 75 30
26

FIGURE 10.b.

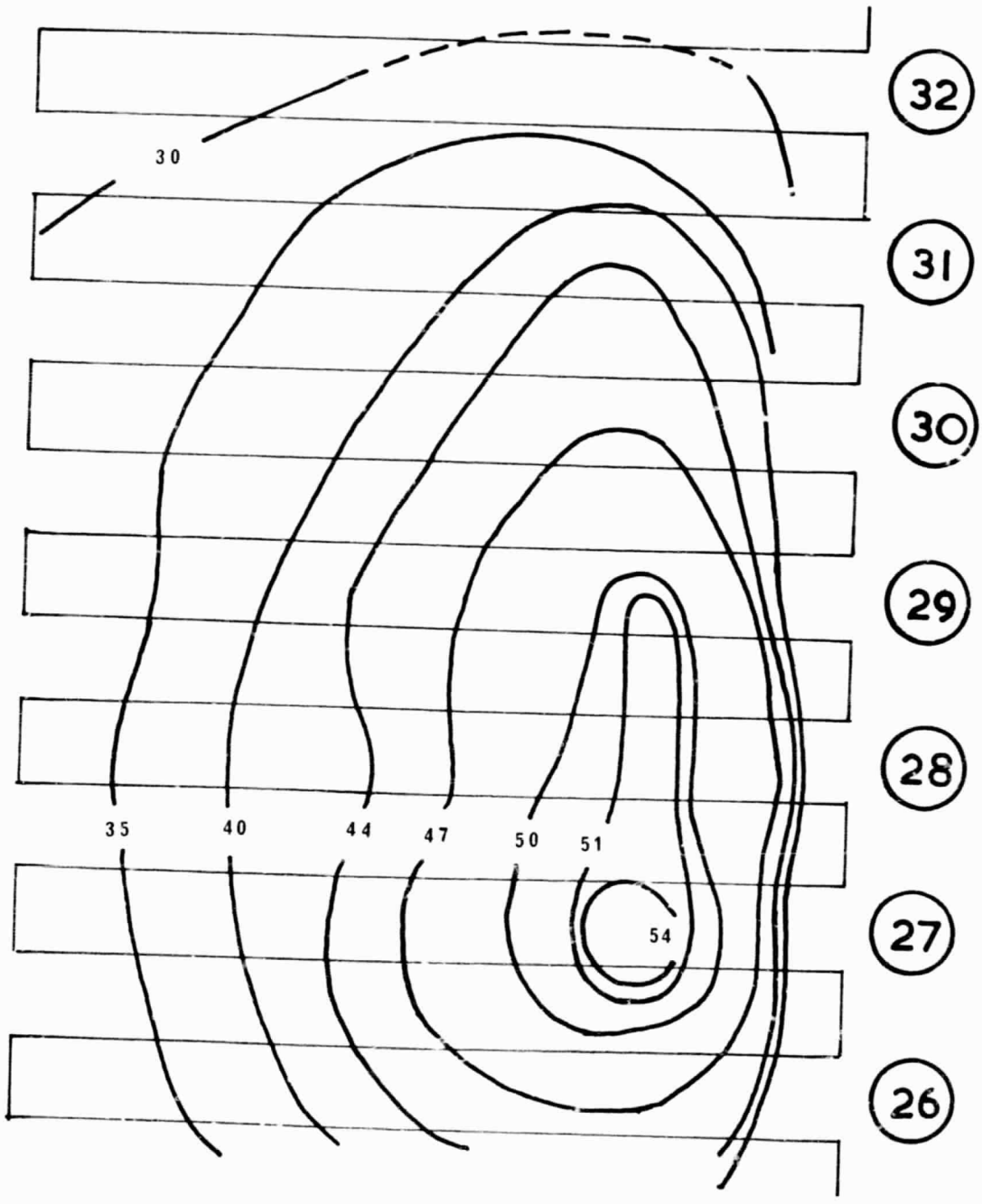

FIGURE II.a.

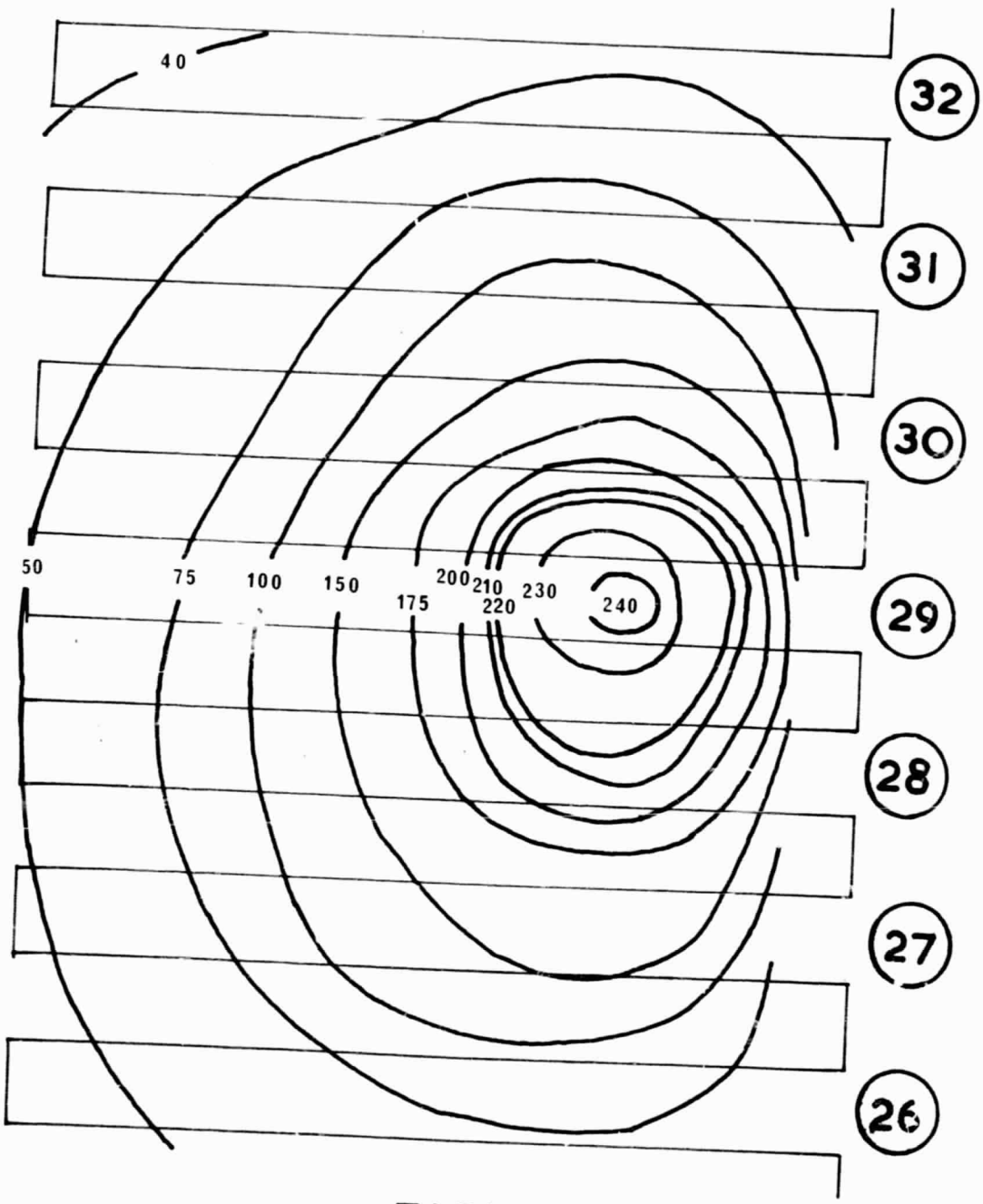

FIGURE II.b.

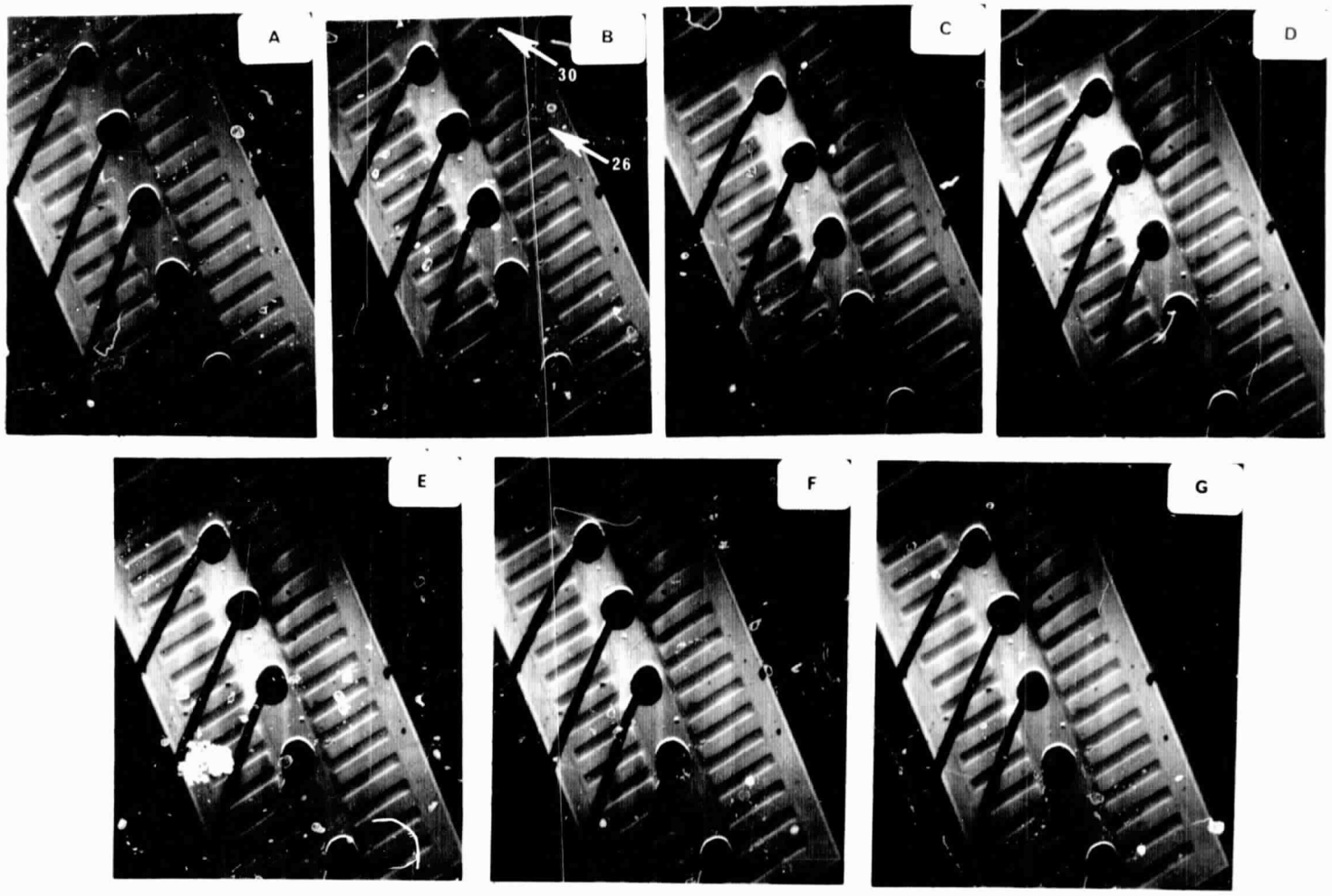

FIGURE.12.

FIGURE 13

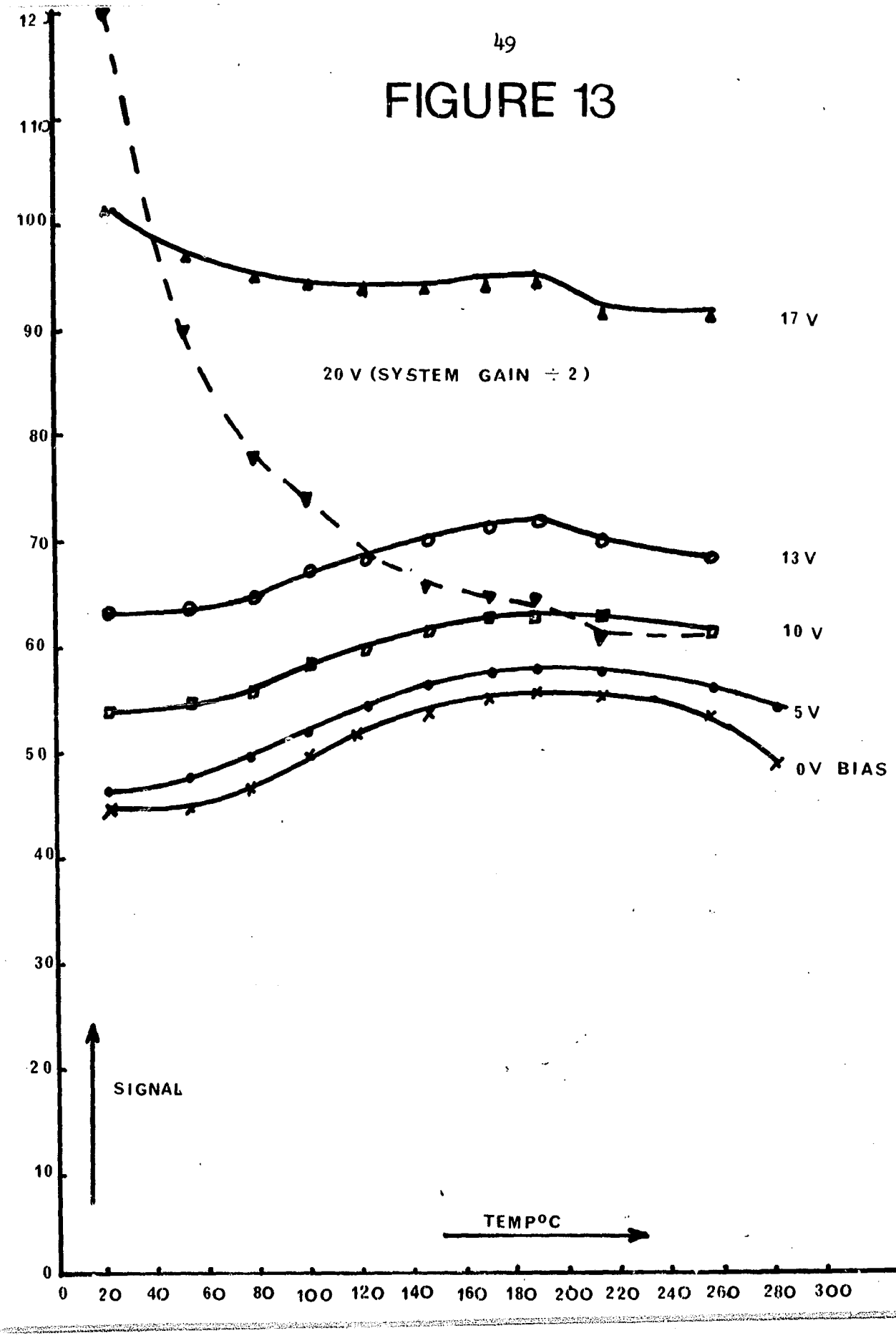
12
110
100
90
80
70
60
50
40
30
20
10
0
17 V
20 V (SYSTEM GAIN ÷ 2)
13 V
10 V
5 V
0V BIAS
SIGNAL
TEMP°C
0 20 40 60 80 100 120 140 160 180 200 220 240 260 280 300

University College of North Wales
Grant NGR-52-117-001

Applications (4). Application to assessment of ion implanted diodes

1. Introduction

In devices which are free of gross inhomogeneities we can use the SEM to study the variations in junction uniformity across the junction. This method can be made very sensitive if the device is studied under avalanche conditions. If we ignore edge effects and assume that the resistance of the surface skin is so low that the voltage drop across the surface layer is insignificant then we can assume that a constant voltage equal to the applied voltage exists across each element of the junction. Under these conditions a fractional change in junction width, $\frac{\Delta W}{W}$, creates an equal fractional change in the electric field. Since the multiplication is a sensitive function of the local field it is, in this case, a sensitive function of the junction width. To test this idea we studied an ion implanted diode and compared the results obtained with the data available on diffused diodes.

2. Specimen and initial results

The specimen used was an early experimental mesa diode about 400μ in diameter made by implantation of P into n-type Si of resistivity 5Ω cm. The device was examined at room temperature in an ion pumped SEM at a vacuum of 4×10^{-7} torr. The salient features of the

observations are given in figure 1. It should be stressed that these are observations made on an early device and that the technique has improved since its fabrication. The fact that this is an early experimental device leads to two effects which should be clarified at the outset. In figure 1(a) it is seen that there is a dark, 'flow-pattern' like region about the bond. This loss of signal is caused by the bonding method used at that date and in no way reflects on the quality of the junction as made by ion implantation. Secondly, it can be seen that there are regions of signal outside the mesa. These have two origins. One is associated with localised breakdown at the mesa edge and the other is caused by a beam induced inversion of the p-type substrate. These two types can be distinguished on purely geometrical grounds, the edge breakdown occurs randomly round the mesa edge, while the beam induced inversion has essentially rectangular shapes arising from the superposition of several rasters and line scans. Again these effects have no significance in assessing the quality of the junction as made by ion-implantation.

The quality of the ion implanted diode can be judged from the signal within the mesa area. This signal can be seen to be remarkably uniform in figures 1(a) to (c), which were obtained at bias voltages

before the 'knee' in the current-voltage characteristic. Figure 1(d) was obtained at or about the 'knee' which occurs at about 140V. Figures 1(e) to (h) were obtained at biases beyond the knee in the curve and do show some variation in signal. In particular there is a region in the bottom centre area which breaks down at a slightly lower voltage than the bulk and which represents the main signal variations. A more detailed examination of the anomalous area showed that a possible cause of the observed behaviour was the presence of two dislocations in the centre of this region. Figures 1(i) and (k) show these defects in more detail at biases of 0, 142 and 145 volts respectively. We cannot be certain that these defects are the cause of the observed variation. To do this we have to make further measurements. Such measurements depend at present on the availability of further devices. Even if these defects are not responsible for the major variation in signal beyond the knee these diodes still compare favourably with those made by diffusion. This fact can be verified by making quantitative studies of the charge collection across the relevant areas.

3. Quantitative studies of the charge collection signal as a function of bias

Figure 2 shows the relative signals obtained along preselected lines on the diode studied in figure 2. The lines along which these

scans were taken are indicated in the line diagram in figure 2(a). It can be seen that prior to breakdown the signal is very uniform, but after breakdown there is a variation which is at the most between 2 and 3 along the lines chosen. These lines include the anomalous area referred to above. At first sight it may appear that devices with spatial variations in junction behaviour of up to 2 to 3 times are not very good. However, the sensitivity of the method should be borne in mind and a comparison with diffused diodes made. With regard to the sensitivity of the method we have shown in the appendix that for abrupt and graded junctions the fractional change in signal, $\frac{\Delta S}{S}$, between two elements of the junction is related to the corresponding change in field, $\frac{\Delta E}{E}$, by the equation

$$\left|\frac{\Delta S}{S}\right| \geq M \times \left|\frac{\Delta E}{E}\right| = M \times \left|\frac{\Delta W}{W}\right| \qquad \text{eq. 1}$$

Therefore factors of 2 and 3 in signal imply values of $\frac{\Delta E}{E}$ $(= \frac{\Delta W}{W})$ of between 2 and 3% as $M \simeq 100$ in these diodes. This figure for the variation can be regarded as satisfactory as crystal resistivity is only constant to this order anyway. The quality of this ion implanted diode can be further tested by comparing it with a diffused diode of good quality.

Figure 3 shows line scans taken of an avalanche diode made by proven techniques (1). Although the diode is about 50 times smaller than the ion implanted diode studied the variations in charge collection signal are larger. Variations of x 10 are not uncommon. With the available data we cannot state that the apparently more uniform behaviour of the ion implanted diode is due to the superiority of the ion implantation technique because the substrates used in the two devices had different resistivities. Even so, bearing in mind that the ion implanted device was made in the higher resisitivity material, it is likely that the improvement is largely due to the ion implantation technique. However, it must be borne in mind that only one such device has been examined to date.

Appendix. The sensitivity of the charge collection signal to variations in junction properties under avalanche conditions.

Under avalanche conditions the charge collection signal, S, from a given element is proportional to the effective multiplication, M. So the difference in signal, ΔS, between two elements is related to the corresponding change in multiplication, ΔM, by

$$\frac{\Delta S}{S} = \frac{\Delta M}{M} \qquad \text{eq. 1}$$

The multiplication can be related to the ionization probability, α, by

$$1 - \frac{1}{M} = \int_0^W \alpha \, dz \qquad \text{eq. 2}$$

where W is the junction width. In the case of interest here we can write α as a function the local field in terms of the expression given by Lee et al (2). For Si we can write

$$\alpha = A \exp\{ -[B/E] \} \qquad \text{eq. 3}$$

with $A = 3.8 \times 10^{+6} (cm^{-1})$; $B = 1.75 \times 10^{6} (V/cm)$ for electrons

$A = 2.25 \times 10^{7} (cm^{-1})$; $B = 3.26 \times 10^{6} (V/cm)$ for holes

With this expression and using equation 2 we obtain

$$1 - \frac{1}{M} = \int_0^W A \exp\{ -\left[B/E(z)\right] \} dz \qquad \text{eq. 4(a)}$$

$$= WA \exp\left[-\left(\frac{BW}{V_{app}}\right)\right] \qquad \text{eq. 4(b)}$$

for a step and graded junction respectively, where V_{app} is the applied voltage. From this equation we obtain

$$\frac{\Delta M}{M} = - M \frac{\Delta W}{W} \frac{\Delta V_{app}}{E_{max}} \exp\left[-\left(\frac{B}{E_{max}}\right)\right] \qquad \text{eq. 5(a)}$$

$$= - KM \frac{\Delta W}{W}$$

for an abrupt junction where E_{max} is the highest field value and

$$\frac{\Delta M}{M} = M \frac{\Delta W}{W} \left(1 - \frac{1}{M}\right) \left[1 - \frac{WB}{V_{app}}\right] \qquad \text{eq. 5(b)}$$

for a graded junction. Examine the case of the graded junction first. Since we are considering situations in which $M >> 1$, $(1 - \frac{1}{M}) \to 1$. Since we are concerned with voltages near $\overline{V_b}$, the diode breakdown voltage we can write $V_{app} = W E_{max} = \overline{V_b}$

Therefore

$$\frac{\Delta S}{S} = \frac{\Delta M}{M} \approx M \frac{\Delta W}{W} \left[1 - \frac{B}{E_{max}}\right] \qquad \text{eq. 6}$$

Because $E_{max} \sim 3.5 \times 10^5$ V/cm for Si diode with a breakdown voltage of 100 volts (4) we have values of 5 and 9.5 for $\frac{B}{E_{max}}$ for electrons

and holes in Si respectively. As E_{max} varies very slowly with doping level (5), we can also taken this value for the second diode studied here which had a breakdown voltage of 20 volts. Therefore we can write

$$\left|\frac{\Delta S}{S}\right| \geq M\left|\frac{\Delta W}{W}\right| \qquad \text{eq. 7}$$

for graded junctions. Similar estimates for the abrupt junction case made using the data in references (3) and (5), indicate that the inequality given in equation 7 is valid for this case as well as for diodes breaking down at both 20 and 100V. These estimates also show that the constant K in equation 5(a) is probably slightly smaller as the breakdown voltage decreases. This result substantiates the claim made in the text that the ion-implanted diode studied is probably more uniform than the diffused diodes examined in this work.

It should be stressed that the analysis given here is approximate and is given only to establish how sensitive the method of examining junction uniformity is. The main approximations are (1) the assumption, inherent in equation 2, that the ionization coefficients for electrons and holes are equal and (2) the tacit assumption in equation 1 that the difference in signal between two surface elements is due entirely to differences in multiplication. This is equivalent to

assuming that the local series resistances are equal or that we are measuring the short circuit current, i.e. that the local series resistances are small. It is intended to analyse this method more fully at a later date.

References

1. See for example, R. H. Haitz, J. Appl. Phys. 36, 3123, (1965).

2. C. A. Lee, R. A. Logan, R. L. Batdorf, J. F. Kleimack and W. Wiegmann, Phys. Rev. 134, A761, (1964).

3. G. Gibbons and S. M. Sze, Solid State Electron., 11, 225, (1968).

4. S. M. Sze and G. Gibbons, Solid State Electron., 9, 831, (1966).

5. S. M. Sze and G. Gibbons, Appl. Phys. Letters, 8, 111, (1966).

Captions to figures

Figure 1. Conductive micrographs of the ion-implanted diode studied in the text. The micrographs were taken under the following bias conditions:

(a) $V_b = 0$
(b) $V_b = 112V$
(c) $V_b = 136.2V, < 1\mu a$
(d) $V_b = 139.6V$, $10\mu a$
(e) $V_b = 141.3V$, $60\mu a$
(f) $V_b = 142.1$, $90\mu a$
(g) $V_b = 143.9$, $160\mu a$
(h) $V_b = 145.6$, $250\mu a$
(i) $V_b = 0$
(j) $V_b \sim 142V$
(k) $V_b \sim 145V$

Figure 2. Line scans taken across the diode studied in figure 1. (a) shows the position of the line scans obtained, (b) line scan taken along line aa' with bias of 130 volts. (c) to (f) were obtained at 140V, 141V; 145.1V, $200\mu a$; 150.7V, $420\mu a$ respectively.

Figure 3. Similar line scans taken on a high quality diffused diode (a) 0 to 5V, (b) 20.07V; (c) 21.17V, $42\mu a$; (d) 21.49V, $270\mu a$ and (e) 21.84V, 0.5ma.

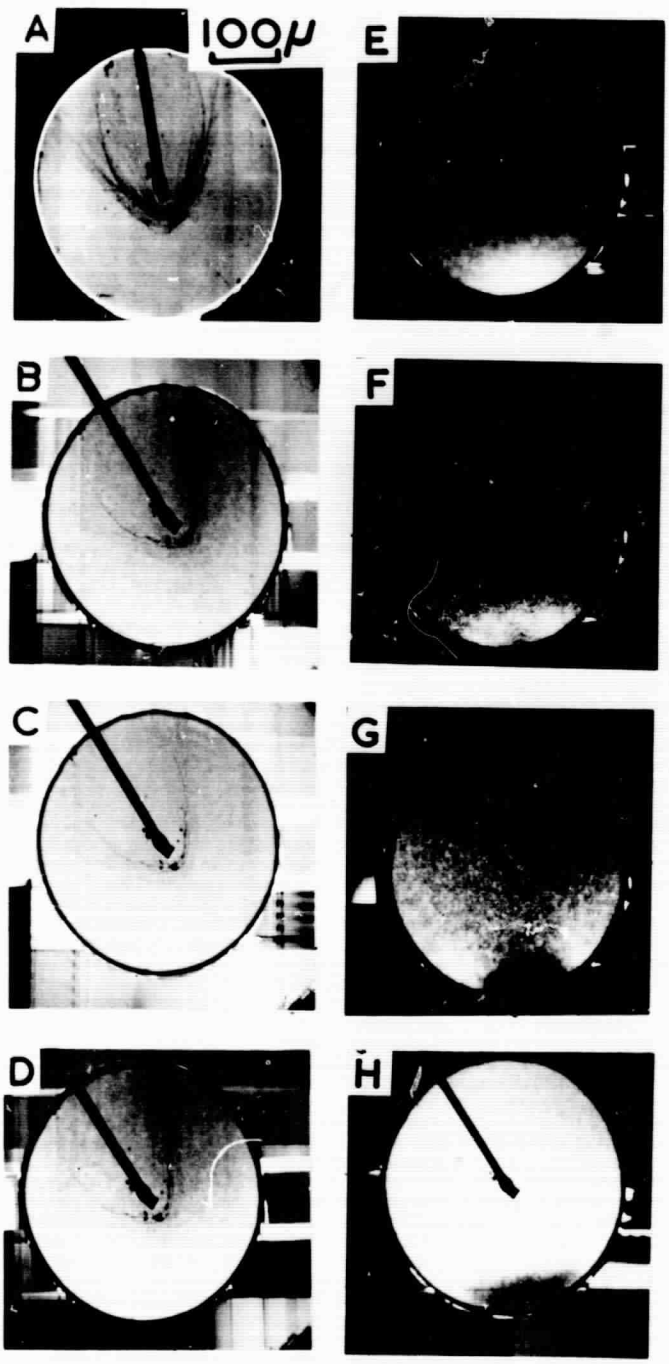

FIGURE 1

FIGURE.2.

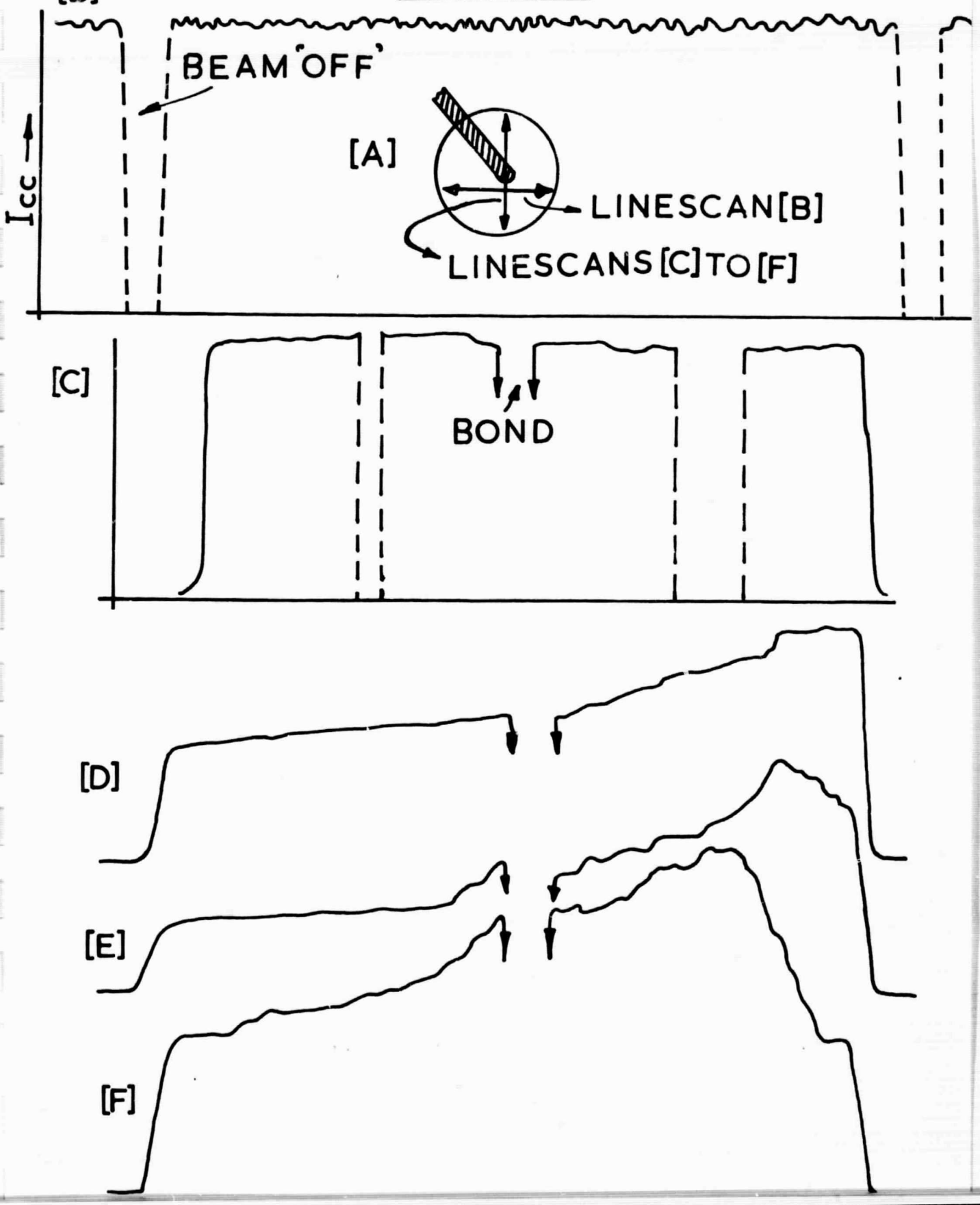

FIGURE.3.

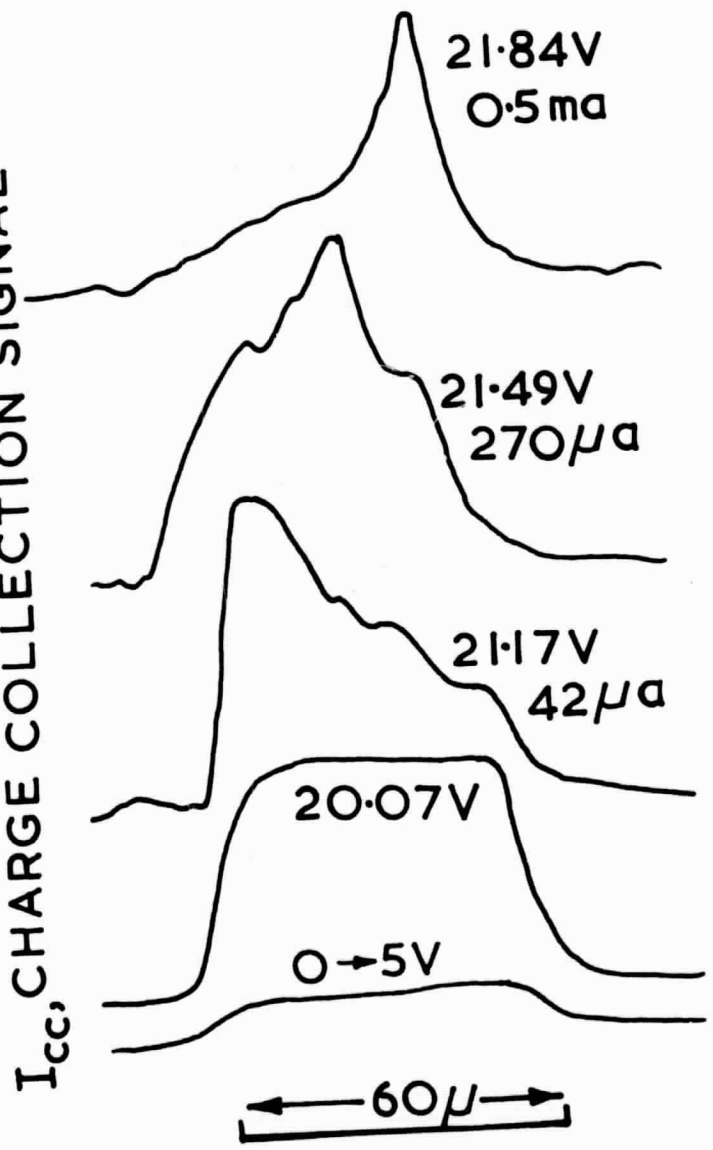
21·84V
0·5 ma
21·49V
270μa
21·17V
42μa
20·07V
0→5V
I_{cc}, CHARGE COLLECTION SIGNAL→
←60μ→